

1 **Measurement report: Source apportionment of carbonaceous aerosol using**  
2 **dual-carbon isotopes (<sup>13</sup>C and <sup>14</sup>C) and levoglucosan in three northern Chinese**  
3 **cities during 2018–2019**

4  
5 Huiyizhe Zhao <sup>a, c, d</sup>, Zhenchuan Niu <sup>a, b, c, d, e, \*</sup>, Weijian Zhou <sup>a, b, c, d, \*</sup>, Sen Wang<sup>f</sup>, Xue  
6 Feng<sup>g</sup>, Shugang Wu <sup>a, c</sup>, Xuefeng Lu <sup>a, c</sup>, Hua Du <sup>a, c</sup>

7 <sup>a</sup> *State Key Laboratory of Loess and Quaternary Geology, CAS Center for Excellence*  
8 *in Quaternary Science and Global Change, Institute of Earth Environment, Chinese*  
9 *Academy of Sciences, Xi'an 710061, China*

10 <sup>b</sup> *Open Studio for Oceanic-Continental Climate and Environment Changes, Pilot*  
11 *National Laboratory for Marine Science and Technology (Qingdao), Qingdao 266061,*  
12 *China*

13 <sup>c</sup> *Shaanxi Provincial Key Laboratory of Accelerator Mass Spectrometry Technology*  
14 *and Application, Joint Xi'an AMS Center between IEECAS and Xi'an Jiaotong*  
15 *University, Xi'an 710061, China*

16 <sup>d</sup> *University of Chinese Academy of Sciences, Beijing 100049, China*

17 <sup>e</sup> *Shaanxi Guanzhong Plain Ecological Environment Change and Comprehensive*  
18 *Treatment National Observation and Research Station, Xi'an, China*

19 <sup>f</sup> *Shaanxi Key Laboratory of Earth Surface System and Environmental Carrying*  
20 *Capacity, College of Urban and Environmental Sciences, Northwest University, Xi'an,*  
21 *China*

22 <sup>g</sup> *Xi'an Institute for Innovative Earth Environment Research, Xi'an, China*

23 **Correspondence:** Zhenchuan Niu (niuzc@ieecas.cn) and Weijian Zhou  
24 (weijian@loess.llqg.ac.cn)

25

26 **Abstract**

27 To investigate the characteristics and changes in the sources of carbonaceous  
28 aerosols in northern Chinese cities after the implementation of the Action Plan for Air  
29 Pollution Prevention and Control in 2013, we collected PM<sub>2.5</sub> samples from three  
30 representative inland cities, viz. Beijing (BJ), Xi'an (XA), and Linfen (LF) from  
31 January 2018 to April 2019. Elemental carbon (EC), organic carbon (OC),  
32 levoglucosan, stable carbon isotope, and radiocarbon were measured in PM<sub>2.5</sub> to  
33 quantify the sources of carbonaceous aerosol, combined with Latin hypercube  
34 sampling. The best estimate of source apportionment showed that the emissions from  
35 liquid fossil fuels contributed  $29.3 \pm 12.7\%$ ,  $24.9 \pm 18.0\%$ , and  $20.9 \pm 12.3\%$  of the  
36 total carbon (TC) in BJ, XA, and LF, respectively, whereas coal combustion  
37 contributed  $15.5 \pm 8.8\%$ ,  $20.9 \pm 18.0\%$ , and  $42.9 \pm 19.4\%$ , respectively. Non-fossil  
38 sources accounted for  $55 \pm 11\%$ ,  $54 \pm 10\%$ , and  $36 \pm 14\%$  of the TC in BJ, XA, and  
39 LF, respectively. In XA,  $44.8 \pm 26.8\%$  of non-fossil sources was attributed to biomass  
40 burning. The highest contributors to OC in LF and XA were fossil sources ( $74.2 \pm 9.6\%$   
41 and  $43.2 \pm 10.8\%$ , respectively), whereas that in BJ was non-fossil sources ( $66.8 \pm$   
42  $13.9\%$ ). The main contributors to EC were fossil sources, accounting for  $91.4 \pm 7.5\%$ ,  
43  $66.8 \pm 23.8\%$ , and  $88.4 \pm 10.8\%$  in BJ, XA, and LF, respectively. The decline (6–16%)  
44 in fossil source contributions in BJ since the implementation of the Action Plan  
45 indicates the effectiveness of air quality management. We suggest that specific  
46 measures targeted to coal combustion, biomass burning and vehicle emissions in  
47 different cities should be strengthened in the future.

48

49 **Keywords:** carbonaceous aerosols; radiocarbon; stable carbon isotope; biomass  
50 burning; fossil fuel combustion; source apportionment

## 51 **1 Introduction**

52 Atmospheric aerosols are extremely complex suspension systems. Carbonaceous  
53 aerosols are an important component of atmospheric aerosols, accounting for  
54 approximately 10–60% of the total mass of global fine particulate matter (Cao et al.,  
55 2003, 2007; Feng et al., 2009). Carbonaceous aerosols contain elemental carbon (EC),  
56 organic carbon (OC), and inorganic carbon (IC). IC is mainly derived from sand dust,  
57 it has a low concentration and simple composition, and it can be removed via acid  
58 treatment (Clarke et al., 1992). EC is produced by incomplete combustion and is  
59 directly discharged from pollution sources. It can cause global warming by changing  
60 the radiative forcing and ice albedo (Jacobson et al., 2001; Kiehl et al., 2007). OC is a  
61 complex mixture of primary and secondary pollutants produced by the combustion of  
62 domestic biomass and fossil fuels. It is an important contributor to tropospheric ozone,  
63 photochemical smog, and rainwater acidification, and it can significantly impact  
64 regional and global environments through biogeochemical cycling (Jacobson et al.,  
65 2000; Seinfeld et al., 1998). Therefore, identifying and quantifying the source  
66 contributions of carbonaceous aerosols can provide a scientific basis for the  
67 management of regional air quality.

68 The natural radiocarbon ( $^{14}\text{C}$ ) is completely depleted in fossil emissions, due to  
69 the age of fossil fuels well above the half-life of  $^{14}\text{C}$  (5730 years), whereas non-fossil  
70 sources show the similar  $^{14}\text{C}$  as environment (Szidat, 2009; Heal, 2014). Therefore,  
71  $^{14}\text{C}$  can be used to study the source of atmospheric particulate matter and to  
72 quantitatively and accurately distinguish the contributions of fossil and non-fossil  
73 sources (Clayton et al., 1955; Currie, 2000; Szidat, 2009). In recent decades, this  
74 method has been widely used to trace non-fossil carbonaceous aerosols in various  
75 regions (Ceburnis et al., 2011; Lewis et al., 2004; Szidat et al., 2009; Vonwiller et al.,

76 2017; Yang et al., 2005; Zhang et al., 2012, 2017a). Stable carbon isotope ( $^{13}\text{C}$ ) is a  
77 useful geochemical marker that can provide valuable information about both the  
78 sources and atmospheric processing of carbonaceous aerosols (López-Veneroni, 2009;  
79 Widory, 2006), and it has been applied in various types of environmental research to  
80 identify emission sources (Cachier et al., 1985, 1986; Cao et al., 2011; Chesselet et al.,  
81 1981; Fang et al., 2017; Kawashima & Haneishi, 2012; Kirillova et al., 2013). The  
82 analysis of  $^{13}\text{C}/^{12}\text{C}$  can refine  $^{14}\text{C}$  source apportionment because both coal and liquid  
83 fossil fuels are depleted of  $^{14}\text{C}$  while their  $^{13}\text{C}$  source signatures are different  
84 (Andersson et al., 2015; Li et al., 2016; Winiger et al., 2017). Levoglucosan (Lev), a  
85 thermal degradation product of cellulose combustion, is a common molecular tracer  
86 that can be used to evaluate the contribution of biomass burning (Hoffmann et al.,  
87 2010; Locker et al., 1988; Simoneit et al., 1999). The combination of the carbon  
88 isotope analysis and Lev can further divide the contributions of different  
89 carbonaceous sources. Some studies have confirmed the feasibility of this  
90 combination (Claeys et al., 2010; Gelencsér et al., 2007; Genberg et al., 2011; Huang  
91 et al., 2014; Kumagai et al., 2010; Liu et al., 2013; Niu et al., 2013; Zhang et al.,  
92 2015).

93 Cities in northern China have been affected by severe haze for several decades  
94 (Cao et al., 2012; Han et al., 2016; Sun et al., 2006; Wang et al., 1990). After the  
95 Action Plan for Air Pollution Prevention and Control (hereafter simplified as “Action  
96 Plan”) was promulgated in 2013, all parts of China responded to the issue and held  
97 numerous air quality management practices (CSC, 2013). In 2020, the average  $\text{PM}_{2.5}$   
98 concentration in Chinese cities across the country decreased by 54.2% compared to  
99 that in 2013 (MEE, 2014, 2021). In 2020, the proportion of clean energy consumption,  
100 such as that of natural gas and electricity, increased by 7.9% compared to that in 2013,

101 and the proportion of coal combustion decreased by 9.7% (NBS, 2021). Before the  
102 Action Plan, fossil fuel sources were identified as the main contributor to  
103 carbonaceous aerosols in Chinese cities (56–81%) (Ni et al., 2018, Niu et al., 2013,  
104 Shao et al., 1996; Sun et al., 2012; Yang et al., 2005). In this study, we aimed to  
105 determine the main contribution of the current carbonaceous aerosols in northern  
106 Chinese cities. Also, we aimed to identify whether changes in energy type and  
107 emission control caused a change in the source of carbonaceous aerosols.

108 To address those issues, we conducted a source apportionment of carbonaceous  
109 aerosols based on yearly measurements of OC, EC, Lev,  $^{13}\text{C}$ , and  $^{14}\text{C}$  in  $\text{PM}_{2.5}$ ,  
110 combined with Latin hypercube sampling (LHS), in three representative northern  
111 Chinese cities during 2018–2019. This study provides a comprehensive understanding  
112 of current sources of carbonaceous aerosol after the implementation of the Action  
113 Plan in Chinese cities.

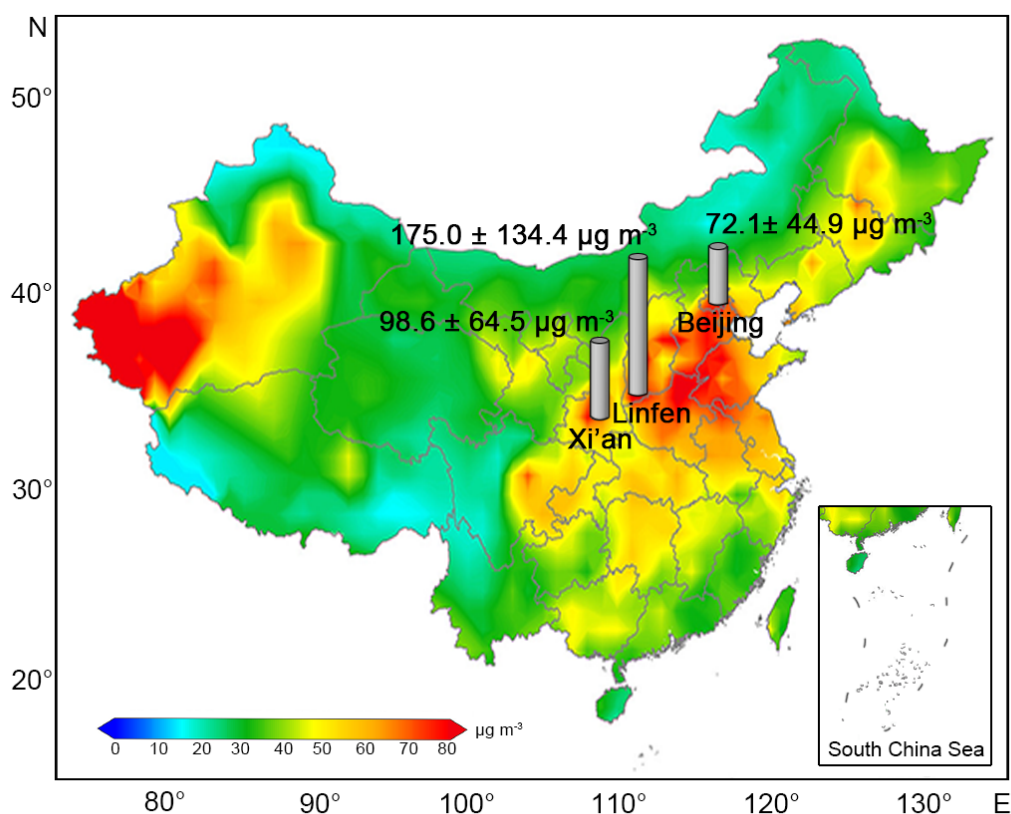
114

## 115 **2 Methods**

### 116 **2.1 Research sites**

117 We selected one urban sampling site in Beijing (BJ), one in Xi'an (XA), and one  
118 in Linfen (LF) (Fig. 1). BJ is the capital of China, one of the largest megacities in the  
119 world, and the central city of the Beijing–Tianjin–Hebei economic region. It has a  
120 population of more than 20 million and has experienced serious air pollution problems  
121 in the past few decades. XA, the capital of Shaanxi Province, is the ninth-largest  
122 central city and an important city of the Northwest Economic Belt in China. It is  
123 located in a basin surrounded by mountains on three sides, where atmospheric  
124 pollutants are discharged mainly from the basin and are less affected by other urban  
125 areas (Cao et al., 2009; Shen et al., 2011). LF is located in western Shanxi Province

126 and is one of the representative cities in the northern air-polluted region. Shanxi  
127 Province is the center of Chinese energy production and chemical metallurgy  
128 industries; its coal production and consumption were approximately 736.81 million  
129 tons and 349.07 million tons, accounting for 27.1% and 12.4% of the Chinese total in  
130 2019, respectively (NBS, 2020; SPBS, 2020). The air quality in LF was ranked in the  
131 worst ten in China from 2018 to 2020 (MEE, 2019, 2020, 2021). According to the  
132 pollutant data released by the National Air Quality Real-time Release Platform,  
133 Ministry of Ecology and Environment (MEE) of the People's Republic of China  
134 (<http://106.37.208.233:20035/>), the daily average atmospheric SO<sub>2</sub> concentration in  
135 LF exceeded 850 μg m<sup>-3</sup> on January 4<sup>th</sup>, 2017. XA and LF heavily suffer from air  
136 pollution in the Fenwei Plain. In July 2018, the State Council issued the Three-Year  
137 Action Plan to Win the Blue Sky Defense War. This included the Fenwei Plain as one  
138 of the key areas in which to prevent and control pollution (CSC, 2018).



139

140 Fig. 1 Locations and PM<sub>2.5</sub> concentration of Beijing (BJ), Xi'an (XA), and Linfen  
141 (LF). The background map shows the distribution of PM<sub>2.5</sub> concentrations in most of  
142 China from 2015 to 2019 (Li et al., 2021a). The gray bars are the average PM<sub>2.5</sub>  
143 concentrations of the samples collected in this study during 2018 to 2019.

144 The first site was located in the northwest of BJ, on the rooftop of the Research  
145 Center for Eco-Environmental Sciences, Chinese Academy of Sciences (40°0'33" N,  
146 116°20'38" E). The site was approximately 200 m from the road. The second site was  
147 located southwest of XA, on the rooftop of the School of Urban and Environmental  
148 Sciences in Northwest University (34°15'36" N, 108°88'53" E). Living quarters and  
149 teaching areas were located around these two sampling sites. The third site was  
150 located in Houma, a county-level city of LF, on the rooftop of a residential building  
151 (35°63'56" N, 111°39'53" E). There was no industrial pollution near each site and  
152 they were representative urban sites.

153

## 154 **2.2 Sample collection**

155 At BJ and XA, PM<sub>2.5</sub> samples were collected on the 7<sup>th</sup>, 14<sup>th</sup>, 21<sup>st</sup>, and 28<sup>th</sup> of  
156 each month from April 28, 2018, to April 21, 2019. In LF, seven consecutive days in  
157 each season were selected for sample collection, and the sampling periods were  
158 concentrated in January, April, July, and October 2018. A total of 124 24-hour (10  
159 a.m. to 10 a.m. on the following day) PM<sub>2.5</sub> samples and 4 field blanks were obtained.

160 Samples in each city were collected continuously on pre-baked quartz fiber  
161 filters (203 mm × 254 mm, Whatman UK) using a high-volume (1.05 m<sup>3</sup> min<sup>-1</sup>)  
162 sampler (TH-1000CII). The sampler was equipped with an impact collector to collect  
163 the particles less than 2.5 μm in aerodynamic diameter. To remove the existing carbon  
164 in the materials, the filter and foil used for wrapping should be baked in a muffle

165 furnace at 375 °C for 5 h before use. After sampling, the filters were folded, wrapped  
166 in pre-baked aluminum foil, and stored at -18 °C. All filters were weighed after  
167 equilibrating at 25 ± 1 °C and 52 ± 5% humidity for more than 24 h. The PM<sub>2.5</sub> mass  
168 loadings were determined gravimetrically using a 0.1 mg sensitivity electronic  
169 microbalance. Carbonate has been removed from the filters by spraying with  
170 hydrochloric acid (1 mol L<sup>-1</sup>) before measurement.

### 171 **2.3 OC and EC analyses**

172 Filter pieces of 0.526 cm<sup>2</sup> were used to measure the OC and EC using a DRI  
173 Model 2001 (Thermal/Optical Carbon Analyzer) at the Institute of Earth Environment,  
174 Chinese Academy of Sciences. The Interagency Monitoring of Protected Visual  
175 Environments (IMPROVE) thermal/optical reflectance protocol must be followed  
176 because OC and EC have different oxidation priorities under different temperatures  
177 (Cao et al., 2007; Chow & Watson, 2002). OC and EC were defined as OC1 + OC2 +  
178 OC3 + OC4 + OP and EC1 + EC2 + EC3 - OP, respectively, in accordance with the  
179 IMPROVE protocol (Chow et al., 2004). Sample analysis results were corrected by  
180 the average blank and standard sucrose concentrations of OC and EC, respectively.

### 181 **2.4 Lev analysis**

182 The molecular tracer (Lev) was determined by high-performance anion exchange  
183 chromatography with pulsed amperometric detection (HPAEC-PAD) method at the  
184 South China Institute of Environmental Science, Ministry of Ecology and  
185 Environment. A quartz filter sample (2 cm<sup>2</sup>) was extracted with 3 ml of deionized  
186 water in a prebaked glass bottle under ultrasonic agitation and was subsequently  
187 analyzed using a Dionex ICS-3000 system after filtration. The separation requires an  
188 equilibrium period, isocratic elution, and gradient elution. (For a specific description,  
189 refer to Zhang et al., 2013.) The instrument sample loop was 100 µL and the detection



190 limit of Lev was  $1 \times 10^{-8} \mu\text{g ml}^{-1}$ .

191 Recent studies indicated that Lev was degraded to some extent during  
192 atmospheric transportation, and about 25% of them came from other non-biomass  
193 burning sources (Hoffmann et al., 2010; Wu et al., 2021). Therefore, correction of the  
194 biomass burning source lev ( $\text{Lev}_{\text{bb}}$ ) is required before the source apportionment:

$$195 \quad \text{Lev}_{\text{bb}} = \frac{\text{Lev} \times 0.75}{p} \quad (1)$$

196 where  $p$  (0.4–0.65) is the degradation rate of Lev, which has different  
197 characteristics in each season. For specific  $p$  value in each season, please refer to the  
198 research of Li et al. (2021b).

## 199 **2.5 Stable carbon isotope analysis**

200 The  $^{13}\text{C}$  compositions were determined using a gas isotopic analyzer (Picarro  
201 G2131-i) in conjunction with an elemental analyzer (Elemental Combustion System  
202 4010) at the Institute of Earth Environment, Chinese Academy of Sciences.  
203 Specifically, 0.2–0.4 mgC of sample has been placed in a precombusted tin capsule  
204 ( $6 \times 10$  mm) and the air was removed by squeezing. The samples were tested at 980 °C  
205 and 650 °C with 70–80 ml min<sup>-1</sup> helium as the carrier gas and 20–30 ml min<sup>-1</sup> oxygen  
206 as the reaction gas. The resulting gas mixture was then collected in Gas Isotopic  
207 Analyzer (Bachar et al., 2020). Urea standard (CAS Number: 57-13-6) was used as  
208 standard sample.  $^{13}\text{C}$  data are expressed in delta notation with respect to Vienna Pee  
209 Dee Belemnite (VPDB) (Coplen, 1996):

$$210 \quad \delta^{13}\text{C} = \left[ \frac{^{13}\text{C}/^{12}\text{C}_{\text{Sample}}}{^{13}\text{C}/^{12}\text{C}_{\text{VPDB}}} - 1 \right] \times 1000\text{‰} \quad (2)$$

## 211 **2.6 Radiocarbon analysis**

212 The  $^{14}\text{C}$  samples were prepared and tested in the laboratory of Xi'an accelerator  
213 mass spectrometer (AMS) Center. The processed sample was packed in a sealed

214 quartz tube with a silver wire and excessive CuO. The solid sample was then  
215 combusted at 850 °C for 2.5 h to convert it into gas after the vacuum degree was less  
216 than  $5 \times 10^{-5}$  mbar. The gas sample was passed through a liquid nitrogen cold trap  
217 ( $-196$  °C) to freeze CO<sub>2</sub> and water vapor, and then passed through an ethanol–liquid  
218 nitrogen cold trap ( $-90$  °C) to remove water vapor and purify CO<sub>2</sub> (Turnbull et al.,  
219 2007; Zhou et al., 2014). The collected CO<sub>2</sub> was reduced to graphite via a reduction  
220 reaction with zinc particles and iron powder as the reductant and catalyst, respectively  
221 (Jull, 2007; Slota et al., 1987). The graphite was pressed into an aluminum holder and  
222 measured using a 3 Megavolt AMS, with a precision of 3‰ (Zhou et al., 2006, 2007).  
223 Forty-nine targets were arranged in sequence in the sample fixed wheel, including  
224 forty samples, six OX-II standard samples, two anthracite standard samples and one  
225 sugar carbon standard sample each time. AMS online  $\delta^{13}\text{C}$  of was used for isotope  
226 fractionation correction.

227 The <sup>14</sup>C results were expressed as a fraction of modern carbon ( $f_M$ ) (Currie, 2000;  
228 Mook & Plicht, 1999). It defines as the <sup>14</sup>C/<sup>12</sup>C ratio of the sample related to the  
229 isotopic ratio of the reference year 1950 (Stuiver & Polach, 1977):

$$230 \quad f_M = (^{14}\text{C}/^{12}\text{C}_{\text{Sample}})/(^{14}\text{C}/^{12}\text{C}_{1950}). \quad (3)$$

231 Atmospheric nuclear bomb tests in the late 1950s and the early 1960s released a  
232 large amount of <sup>14</sup>C, and the ratio of <sup>14</sup>C/<sup>12</sup>C in atmospheric CO<sub>2</sub> roughly doubled in  
233 the mid-1960s (Hua & Barbetti, 2004; Levin et al., 2003, 2010; Lewis et al., 2004;  
234 Niu et al., 2021). However,  $f_M$  in the atmosphere has been decreasing because of the  
235 dilution effect produced by the absorption of marine and terrestrial biospheres and the  
236 release of fossil fuels. In recent years, studies on background <sup>14</sup>CO<sub>2</sub> in China and  
237 other countries have shown that the  $f_M$  value in the atmosphere has decreased and  
238 approached 1 (Hammer et al., 2017; Niu et al., 2016). This means that the impact of

239 the nuclear explosions has almost disappeared for current atmosphere, and the change  
 240 in current atmospheric  $^{14}\text{C}$  was mainly influenced by the regional natural carbon cycle  
 241 and fossil fuel  $\text{CO}_2$  emissions. Thus, the  $f_{\text{M}}$  values were not corrected in this study,  
 242 because the material used for biomass burning in China was mainly from crop straw  
 243 (Fu et al., 2012; Street et al, 2003b; Yan et al., 2006; Zhang et al., 2017b), and the  
 244 influence of atmospheric nuclear bomb test has basically vanished for the annual  
 245 plants.

246 Non-fossil fractions ( $f_{\text{nf}}$ ) and fossil fractions ( $f_{\text{f}}$ ) were determined from the  $f_{\text{M}}$   
 247 values.

$$248 \quad f_{\text{nf}} = f_{\text{M}} \times 100\% \quad (4)$$

$$249 \quad f_{\text{f}} = (1 - f_{\text{M}}) \times 100\% \quad (5)$$

## 250 **2.7 Source apportionment of total carbon using $^{14}\text{C}$ and $^{13}\text{C}$**

251 To study the contribution of each fossil source to the total carbon (TC), we used  
 252 the principle of isotopic chemical mass balance to further separate fossil sources into  
 253 liquid fossil fuels and coal. Since the amount of carbonaceous aerosol produced by  
 254 natural gas is very low compared to coal and liquid fossil combustion, its contribution  
 255 was not considered here (Chen et al., 2005; England et al., 2002; Guo et al., 2014; Yan  
 256 et al., 2010). In this part,  $^{13}\text{C}$  and  $^{14}\text{C}$  were combined to calculate the contributions of  
 257 non-fossil, coal, and liquid fossil sources.

$$258 \quad f_{\text{nf}} \times \delta^{13}\text{C}_{\text{nf}} + f_{\text{coal}} \times \delta^{13}\text{C}_{\text{coal}} + f_{\text{liq.fossil}} \times \delta^{13}\text{C}_{\text{liq.fossil}} = \delta^{13}\text{C}_{\text{sample}} + \beta \quad (6)$$

$$259 \quad f_{\text{coal}} + f_{\text{liq.fossil}} = f_{\text{f}} \quad (7)$$

260 where  $f_{\text{nf}}$ ,  $f_{\text{coal}}$ , and  $f_{\text{liq.fossil}}$  represent the proportions of non-fossil source, coal and  
 261 liquid fossil combustion, respectively,  $\delta^{13}\text{C}_{\text{nf}}$ ,  $\delta^{13}\text{C}_{\text{coal}}$ , and  $\delta^{13}\text{C}_{\text{liq.fossil}}$  represent  $\delta^{13}\text{C}$   
 262 from the corresponding sources.  $\delta^{13}\text{C}_{\text{sample}}$  is the  $\delta^{13}\text{C}$  of the samples at each site, and  
 263  $\beta$  is a small correction.

264 Since the formation process of OC can cause the fractionation of  $^{13}\text{C}$ , with a  
 265 range mainly in 0.03–1.40 ‰ (mean 0.2‰) (Aggarwal and Kawamura, 2008; Cao et  
 266 al, 2011; Ho et al., 2006; Zhao et al., 2018), a small correction (0.2‰) was made for  
 267 the  $\delta^{13}\text{C}$  sample used in Eq. 6. The selection of the reference value was described in  
 268 detail in Section 2.9.

## 269 **2.8 Source apportionment of OC and EC using $^{14}\text{C}$ and $\text{Lev}_{\text{bb}}$**

270 The method combines  $^{14}\text{C}$  with the concentration of carbon components and a  
 271 molecular tracer ( $\text{Lev}_{\text{bb}}$ ) to quantify the sources of OC and EC. Carbon was assumed  
 272 to originate from fossil fuel combustion, biomass burning, and other non-fossil  
 273 emissions (Gelencsér et al., 2007). The following is a simple calculation method.

274 EC consists of biomass burning ( $\text{EC}_{\text{bb}}$ ) and fossil fuel combustion ( $\text{EC}_{\text{ff}}$ ).

$$275 \text{EC} = \text{EC}_{\text{ff}} + \text{EC}_{\text{bb}} \quad (8)$$

276  $\text{EC}_{\text{bb}}$  was calculated based on the  $\text{Lev}_{\text{bb}}$  concentration and the estimated  
 277  $\text{EC}_{\text{bb}}/\text{Lev}_{\text{bb}}$  ratio:

$$278 \text{EC}_{\text{bb}} = \text{Lev}_{\text{bb}} \times (\text{EC}_{\text{bb}}/\text{Lev}_{\text{bb}}) = \text{Lev}_{\text{bb}} \times [(\text{EC}/\text{OC})_{\text{bb}}/(\text{Lev}_{\text{bb}}/\text{OC}_{\text{bb}})] \quad (9)$$

279 Then,  $\text{EC}_{\text{ff}}$  was calculated by subtraction (Eq. 8).

280 OC consists of OC from biomass burning ( $\text{OC}_{\text{bb}}$ ), fossil fuel combustion ( $\text{OC}_{\text{ff}}$ ),  
 281 and other sources ( $\text{OC}_{\text{other}}$ ), including primary and secondary biogenic OC and SOC  
 282 (secondary organic carbon) from non-fossil emissions.

$$283 \text{OC} = \text{OC}_{\text{bb}} + \text{OC}_{\text{ff}} + \text{OC}_{\text{other}} \quad (10)$$

284  $\text{OC}_{\text{bb}}$  was calculated based on the  $\text{Lev}_{\text{bb}}$  concentration and the estimated  
 285  $\text{Lev}_{\text{bb}}/\text{OC}_{\text{bb}}$  ratio:

$$286 \text{OC}_{\text{bb}} = \text{Lev}_{\text{bb}}/(\text{Lev}_{\text{bb}}/\text{OC}_{\text{bb}}) \quad (11)$$

287  $\text{OC}_{\text{other}}$  was calculated by balancing the  $^{14}\text{C}$  content that was not attributed to  
 288  $\text{OC}_{\text{bb}}$ .

289 
$$OC_{\text{other}} = (OC \times f_{\text{nf(OC)}} - OC_{\text{bb}} \times f_{\text{M(bb)}}) / f_{\text{M(nf)}}. \quad (12)$$

290 Furthermore,  $f_{\text{nf(OC)}}$  was calculated based on the  $^{14}\text{C}$  concentration measured in  
291 the sample (detailed description of the formulas can be found in Genberg et al., 2011);  
292  $f_{\text{M(bb)}}$  and  $f_{\text{M(nf)}}$  are the  $^{14}\text{C}$  concentrations in biomass burning and other non-fossil  
293 emissions, respectively.

294 Finally,  $OC_{\text{ff}}$  was calculated by subtraction (Eq. 10).

## 295 **2.9 Uncertainties of source apportionment**

296 Some uncertainties exist in some parameters in Eqs. 5–11 and need to be  
297 evaluated. Table 1 lists the range of reference values used in this study. The ratios  
298  $Lev_{\text{bb}}/OC_{\text{bb}}$  and  $EC_{\text{bb}}/OC_{\text{bb}}$  depend on the type of biofuel and the burning conditions  
299 (Oros et al., 2001a, b). In foreign studies, the most common distributions of  
300  $Lev_{\text{bb}}/OC_{\text{bb}}$  and  $EC_{\text{bb}}/OC_{\text{bb}}$  are 0.08–0.2 and 0.07–0.45, respectively (Gelencsér et al.,  
301 2007; Puxbaum et al., 2007; Szidat et al., 2006). The distribution ranges of  
302  $Lev_{\text{bb}}/OC_{\text{bb}}$  and  $EC_{\text{bb}}/OC_{\text{bb}}$  burned by trees, shrubs, and rice are approximately  
303 0.01–0.04 and 0.05–0.31, respectively (Engling et al., 2006, 2009; Wang et al., 2009).  
304 Zhang et al. (2007) found that the values of  $Lev_{\text{bb}}/OC_{\text{bb}}$  and  $EC_{\text{bb}}/OC_{\text{bb}}$  in the cereal  
305 straw of BJ were 0.08 and 0.13, respectively.

306 The  $\delta^{13}\text{C}$  of aerosols derived from liquid fossil fuels (gasoline and diesel oil) was  
307 approximately  $-31\text{‰}$  to  $-25\text{‰}$  (Agnihotri et al., 2011; Huang et al., 2006;  
308 Lopez-Veneroni, 2009; Pugliese et al., 2017; Vardag et al., 2015; Widory, 2006). The  
309  $\delta^{13}\text{C}$  derived from coal combustion was relatively high, ranging from  $-25\text{‰}$  to  $-21\text{‰}$   
310 (Agnihotri et al., 2011; Pugliese et al., 2017; Widory, 2006). The results of Agnihotri  
311 et al. (2011) showed that the  $\delta^{13}\text{C}$  characteristic of biomass burning emissions ranged  
312 from  $-25.9\text{‰}$  to  $-29.4\text{‰}$ . Smith & Epstein (1971) found that plants with C3 (e.g.,  
313 wheat, soybeans, and most woody plants) and C4 (e.g., corn, grass, and sugar cane)

314 metabolism had significantly different  $\delta^{13}\text{C}$ , with an average of  $-27\text{‰}$  and  $-13\text{‰}$ ,  
 315 respectively. In other studies, these two types of plant-derived aerosols had different  
 316 characteristics; the  $^{13}\text{C}$  from C3 and C4 plants ranged from approximately  $-23.9\text{‰}$  to  
 317  $-32\text{‰}$  (Moura et al., 2008; Turekian et al., 1998) and from  $-11.5\text{‰}$  to  $-13.5\text{‰}$   
 318 (Martinelli et al., 2002), respectively.

**Table 1. Values with limits of input parameters for source apportionment using Latin hypercube sampling (LHS).**

Parameters	Low	Probable value	High
$\text{Lev}_{\text{bb}}/\text{OC}_{\text{bb}}$	0.01	0.11	0.20
$\text{EC}_{\text{bb}}/\text{OC}_{\text{bb}}$	0.13	0.22	0.31
$\delta^{13}\text{C}_{\text{liq.fossil}} (\text{‰})$	$-31.00$	$-27.00$	$-25.00$
$\delta^{13}\text{C}_{\text{Coal}} (\text{‰})$	$-25.00$	$-22.95$	$-21.00$
$\delta^{13}\text{C}_{\text{nf}}^{\text{a}} (\text{‰})$	$-26.00$	$-25.25$	$-24.00$
$\delta^{13}\text{C}_{\text{nf}}^{\text{b}} (\text{‰})$	$-27.00$	$-26.50$	$-25.00$

Agnihotri et al., 2011; Engling et al., 2006, 2009; Gelencs  et al., 2007; Huang et al., 2006; Lopez-Veneroni, 2009; Martinelli et al., 2002; Moura et al., 2008; Oros et al., 2001a, b; Puxbaum et al., 2007; Smith & Epstein, 1971; Szidat et al., 2006; Turekian et al., 1998; Wang et al., 2009; Widory, 2006; Zhang et al., 2007.

<sup>a</sup> Values used in BJ/LF

<sup>b</sup> Values used in XA

319 Because of the differences in the structure of biomass fuels in different cities, we  
 320 selected the  $\delta^{13}\text{C}$  value based on the current status of biomass fuel used in research  
 321 regions. In China, biomass fuels mainly include crop residues, branches, and leaves,  
 322 and the amount of perennial wood is quite small (Zhang et al., 2015). BJ has a small  
 323 area of arable land, with low agricultural output and corn production (BJMBS, 2020).

324 The neighboring province, Hebei, is a large agricultural province that produces a large  
325 amount of wheat and corn annually; the latter has a larger sown area (PGHP, 2020).  
326 Shanxi Province also mainly produces wheat and corn; however, the sown area of  
327 corn is more than three times that of wheat (SPBS, 2020). Agricultural production in  
328 XA and the surrounding Guanzhong area is relatively large. The agricultural structure  
329 is dominated by wheat and corn, and their sown areas are not very different (SAPBS,  
330 2020). This shows that the  $\delta^{13}\text{C}$  of agricultural straw burning in LF is likely to be  
331 higher and that in XA may be lower. Some studies considered that  $\delta^{13}\text{C}$  used for  
332 quantitative mass–balance source apportionment calculations from biomass burning  
333 should mainly be defined as C3 plants (Anderson et al., 2015; Fang et al., 2017; Ni et  
334 al., 2020). Based on this information, the  $\delta^{13}\text{C}$  value of biomass burning in BJ and LF  
335 was found to be approximately  $-26\text{‰}$  to  $-24\text{‰}$ , and that in XA is likely to be from  
336 approximately  $-27\text{‰}$  to  $-25\text{‰}$ . According to the researches about biomass burning  
337 type, perennial biomass fuel was less frequently used in China (Fu et al., 2012; Street  
338 et al, 2003b; Yan et al., 2006; Zhang et al., 2017b), the impact of nuclear explosions  
339 on  $^{14}\text{C}$  data can be ignored, and the  $f_{\text{M}(\text{nf})}$  and  $f_{\text{M}(\text{bb})}$  of the local station should be close  
340 to the atmospheric value.

341 To evaluate the uncertainties of the quantification of source contributions, which  
342 resulted from the uncertainties of the parameters used, we used Python software to  
343 generate 3000 random variable simulations based on the LHS method (Gelencsér et  
344 al., 2007). After excluding part of the out-of-range data, the median value of the  
345 remaining simulations of each sample were considered as the best estimate. The  
346 results of the uncertainties analysis had been discussed further in Section 3.6.

## 347 **2.10 Air mass backward trajectory analysis**

348 For Backward trajectory analysis, air-mass back trajectories from the previous 48

349 h were determined by using the HYbrid Single-Particle Lagrangian Integrated  
350 Trajectory (HYSPLIT) model (Draxler and Hess, 1998) at three different endpoint  
351 heights (e.g., 100 m, 500 m, and 1000 m) and a time interval of 6 h for sampling day  
352 (<https://www.arl.noaa.gov/>).

353

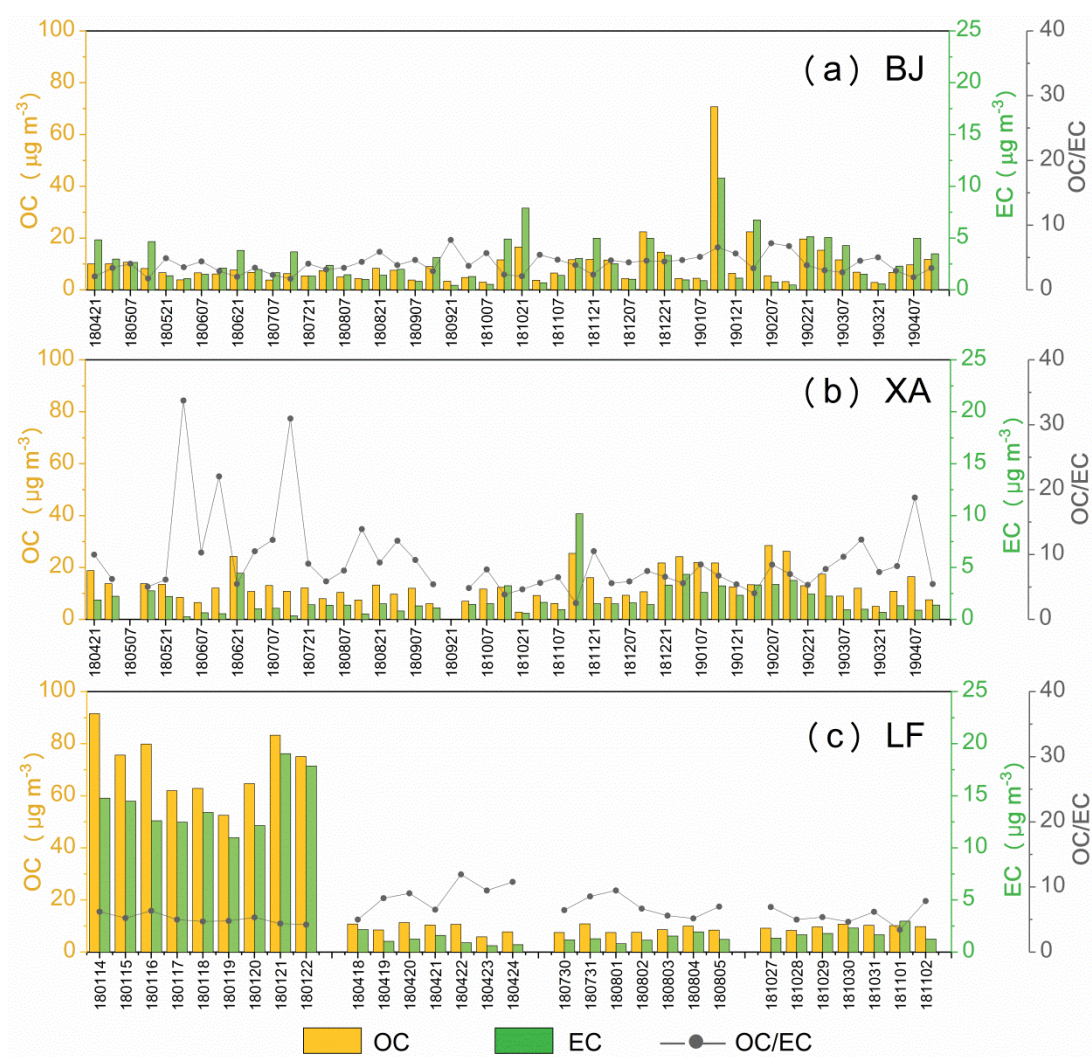
### 354 **3 Results and discussion**

#### 355 **3.1 Characteristics and variation of carbonaceous components**

356 During the sampling period, the average mass concentration of PM<sub>2.5</sub> in BJ, XA,  
357 and LF was  $72.1 \pm 44.9$ ,  $98.6 \pm 64.5$ , and  $175.0 \pm 134.4 \mu\text{g m}^{-3}$ , respectively. All  
358 concentrations were higher in winter and lower in summer; LF showed the highest  
359 value of  $368.7 \pm 75.0 \mu\text{g m}^{-3}$  in winter.

360 Fig. 2 shows the changes in OC and EC and their ratios at the sampling sites. The  
361 carbon components in the BJ, XA, and LF samples accounted for approximately  $17.5$   
362  $\pm 6.0\%$ ,  $21.5 \pm 21.0\%$ , and  $17.8 \pm 7.2\%$  of PM<sub>2.5</sub>, respectively. Both OC and EC were  
363 changing simultaneously and were characterized by low carbonaceous concentrations  
364 in summer (OC:  $8.9 \pm 3.7 \mu\text{g m}^{-3}$ ; EC:  $1.6 \pm 0.9 \mu\text{g m}^{-3}$ ) and high concentrations in  
365 winter (OC:  $69.2 \pm 58.9 \mu\text{g m}^{-3}$ ; EC:  $11.8 \pm 7.9 \mu\text{g m}^{-3}$ ). The average OC/EC ratios in  
366 BJ, XA, and LF were  $4.0 \pm 1.4$ ,  $9.0 \pm 6.1$ , and  $6.6 \pm 2.0$ , respectively. Recent studies  
367 have shown that the average ratio of OC/EC in BJ, XA, and Shanxi Province was  
368 approximately 1.22–6.5 (Han et al., 2016; Ji et al., 2018; Wang et al., 2015; Zhao et  
369 al., 2013). Generally, secondary OC (SOC) is considered to occur when OC/EC > 2  
370 (Castro et al., 1999; Novakov et al., 2005; Turpin & Huntzicker, 1995). Additionally,  
371 the use of biomass fuels can also enhance the OC/EC ratio (Popovicheva et al., 2014;  
372 Rajput et al., 2011). Therefore, the high OC/EC ratio indicates that carbonaceous  
373 aerosols contained a large number of SOCs or biomass burning sources, especially in





375

376 Fig. 2 Variations of elemental carbon (EC), organic carbon (OC) and their ratios in  
 377 PM<sub>2.5</sub> at the sampling sites in Beijing (BJ), Xi'an (XA), and Linfen (LF) (date,  
 378 “yymmdd”).

379 The average mass concentrations of TC, OC, and EC at the sampling site in BJ  
 380 were  $12.5 \pm 11.8$ ,  $9.7 \pm 10.0$ , and  $2.8 \pm 2.1 \mu\text{gC m}^{-3}$ . The concentration of carbon  
 381 components was relatively stable in spring and summer but fluctuated greatly in  
 382 autumn and winter. The concentration of carbon components in most cases was close  
 383 to that of other periods, but there was a rapid increase in autumn and winter. The  
 384 highest TC value was observed in the middle of January 2019 ( $81.5 \mu\text{gC m}^{-3}$ ).

385 The average concentrations of TC, OC, and EC in XA were  $14.6 \pm 7.5$ ,  $12.8 \pm$

386 6.3, and  $1.9 \pm 1.6 \mu\text{gC m}^{-3}$ , respectively. In contrast to that in BJ, the concentration of  
 387 the carbon components in XA fluctuated greatly throughout the year. Specifically, the  
 388 concentration was lower from July to October and significantly higher from  
 389 December to February. However, there were high concentrations of TC on some days  
 390 in spring and summer, such as June 21, 2018, with the concentration reaching 28.8  
 391  $\mu\text{gC m}^{-3}$ .

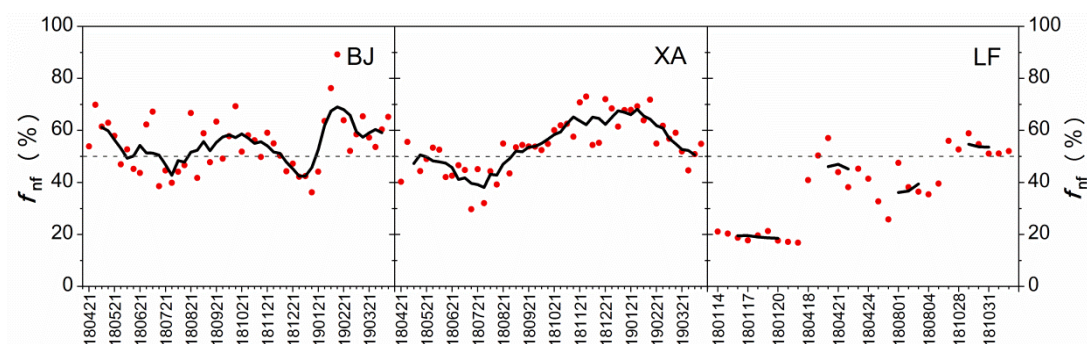
392 The average concentrations of TC, OC, and EC in LF were  $35.7 \pm 36.5$ ,  $30.0 \pm$   
 393  $30.4$ , and  $5.6 \pm 6.2 \mu\text{gC m}^{-3}$ , respectively. In contrast to those in BJ and XA, the  
 394 concentration of the carbon components in LF was persistently high in winter and  
 395 stable and low in other seasons.

396

### 397 3.2 Variations of $^{14}\text{C}$

398 The  $^{14}\text{C}$  results showed that the average  $f_{\text{nf}}$  values in BJ, XA, and LF were  $54 \pm$   
 399  $11\%$ ,  $54 \pm 10\%$ , and  $36 \pm 14\%$ , respectively. Non-fossil sources were the main  
 400 contributors in the BJ and XA samples (Fig. 3). Furthermore, the  $f_{\text{nf}}$  in the BJ samples  
 401 showed a higher average value in spring ( $59 \pm 6\%$ ), whereas that in the XA samples  
 402 had higher average values in autumn ( $f_{\text{nf}}, 59 \pm 7\%$ ) and winter ( $f_{\text{nf}}, 63 \pm 6\%$ ). In the  
 403 LF samples, fossil sources were the main contributors, contributing  $81 \pm 1\%$  in  
 404 winter.

405



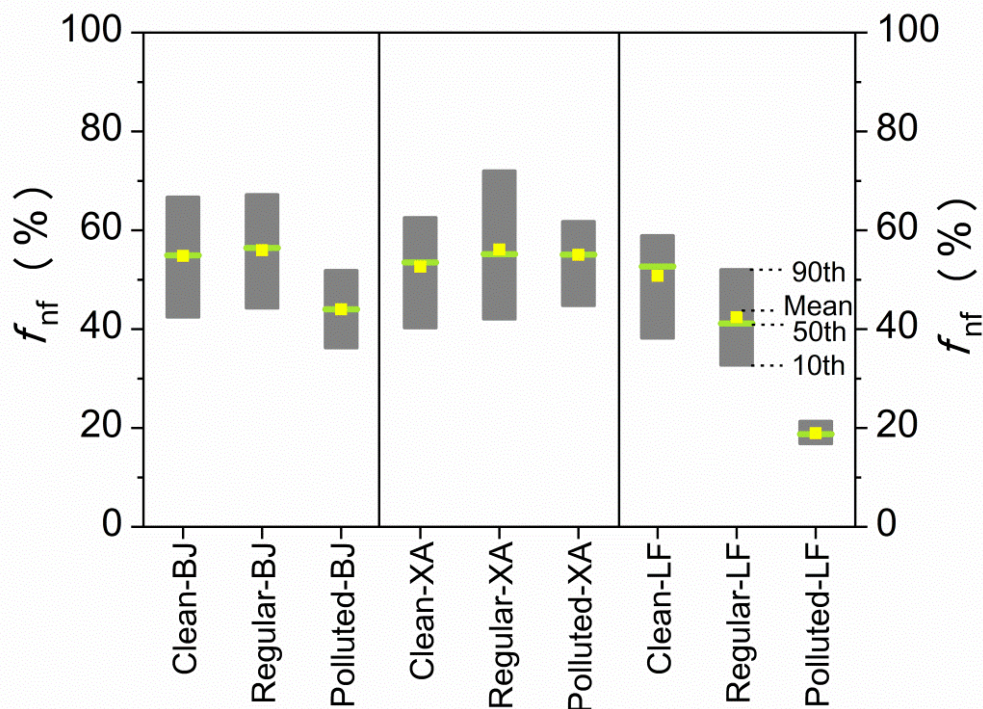
406 Fig. 3 Variations in proportion of non-fossil sources ( $f_{\text{nf}}$ ) of carbonaceous aerosols at

407 the sampling sites in Beijing (BJ), Xi'an (XA), and Linfen (LF). The red scatter dot  
408 represents the  $f_{\text{nf}}$  of each sample, and the black solid line represents the sliding  
409 average  $f_{\text{nf}}$  value of every five samples (date, "yymmdd").

410 By analyzing the  $f_{\text{nf}}$  characteristics of samples with different pollution levels  
411 based on the  $\text{PM}_{2.5}$  concentration, we can study the causes and characteristics of air  
412 pollution more effectively. Using the relevant classification index of the daily average  
413  $\text{PM}_{2.5}$  concentration in the Technical Regulation on Ambient Air Quality Index (MEE,  
414 2012), we divided the samples into clean (with a concentration of less than  $75 \mu\text{g m}^{-3}$ ),  
415 regular (with a concentration between  $75$  and  $150 \mu\text{g m}^{-3}$ ), and polluted (with a  
416 concentration greater than  $150 \mu\text{g m}^{-3}$ ). The  $f_{\text{nf}}$  value in most samples in BJ ( $44 \pm 8\%$ )  
417 and LF ( $19 \pm 2\%$ ) was lower during serious air pollution (Fig. 4), indicating that the  
418 high concentrations of aerosols in BJ and LF were more affected by fossil sources.  
419 One BJ sample had a low  $f_{\text{nf}}$  value (36%) in January and another had a high  $f_{\text{nf}}$  value  
420 (89%) in February. These samples were collected when the atmosphere was severely  
421 polluted and very clean, respectively. This might indicate that emissions from fossil  
422 fuel sources are a decisive factor of air pollution in BJ. In the XA samples, when the  
423 atmosphere was clean,  $f_{\text{nf}}$  decreased by 2–3%, indicating that the carbonaceous  
424 aerosol pollution may be more affected by biomass burning or secondary non-fossil  
425 sources from local emissions.

426 As can be seen in Fig. 5, the contribution of fossil sources in BJ decreased by  
427 about 6–16% for the different sampling season/period after the implementation of  
428 Action Plan, based on previous studies (Fang et al., 2017; Lim et al., 2020; Liu et al.,  
429 2016a, b; Ni et al., 2018, 2020; Shao et al., 1996; Sun et al., 2012; Yang et al., 2005;  
430 Zhang et al., 2015, 2017a) and this study. Among them, fossil sources decreased  
431 significantly in autumn and winter after the Action Plan, which were 15% and 14%,

432 respectively. The contribution of fossil sources in our study decreased by 16% in  
 433 winter compared with the previous results. For the polluted and clean periods, the  
 434 proportion of fossil sources reduced by 6% and 9%, respectively. With the  
 435 implementation of energy conservation and emission reduction policies, many  
 436 non-clean fossil fuels have been replaced by clean energy. In 2019, the coal  
 437 consumption in BJ was only 1.3 million tons, which was 91.5% lower than that in  
 438 2013 (BJMBS, 2020).

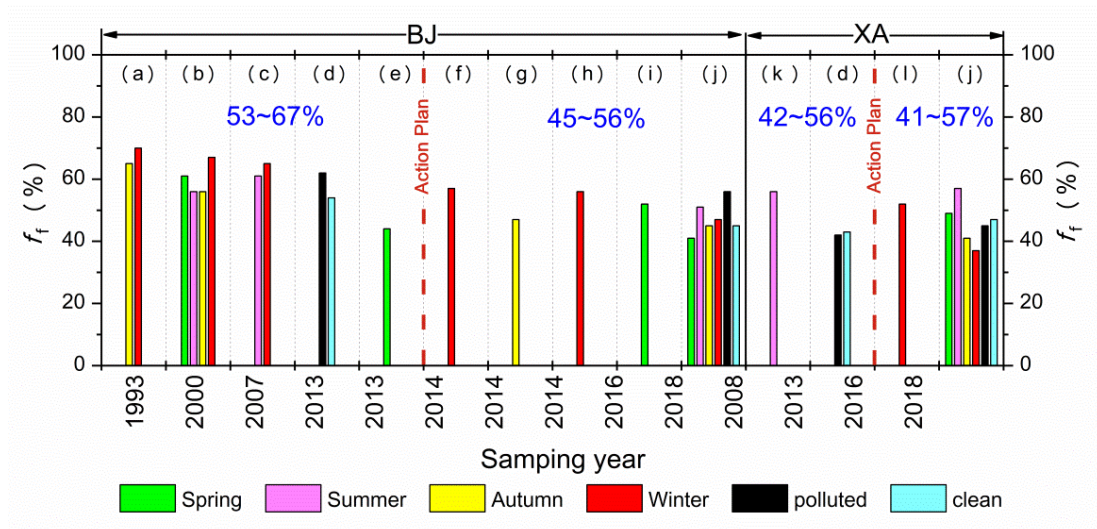


439  
 440 Fig. 4 Box plot distribution of  $f_{nf}$  of samples with different pollution levels. Clean  
 441 samples:  $PM_{2.5} < 75 \mu g m^{-3}$ ; regular samples:  $75 \mu g m^{-3} \leq PM_{2.5} < 150 \mu g m^{-3}$ ;  
 442 polluted samples:  $PM_{2.5} \geq 150 \mu g m^{-3}$ .

443 Different from the results in BJ, the proportion of fossil sources in XA has not  
 444 decreased significantly for each season/period (Fig. 5). This difference might be  
 445 related with a small decline ( $< 0.5\%$ ) in coal consumption in Xi'an during 2019  
 446 compared to 2013 (XAMBS, 2014, 2020). Due to the less attention to LF, there is still



447 a lack of related research of carbonaceous aerosols using radiocarbon in this city to  
 448 compare.



449

450 Fig. 5 Comparison of fossil proportion ( $f_f$ ) of carbonaceous aerosol reported in  
 451 different studies in Beijing (BJ) and Xi'an (XA), China for each season/period. The  
 452 data has been converted to the ratio of total carbon. The ranges shown in the upper  
 453 part of the figure are the average values of each season/period before and after the  
 454 Action Plan. (a) Shao et al., 1996; (b) Yang et al., 2005; (c) Sun et al., 2012; (d)  
 455 Zhang et al., 2015; (e) Liu et al., 2016b; (f) Zhang et al., 2017; (g) Liu et al., 2016a; (h)  
 456 Fang et al., 2017; (i) Lim et al., 2020; (j) This study; (k) Ni et al., 2018; (l) Ni et al.,  
 457 2021.

458

### 459 3.3 Air mass backward trajectory analysis

460 We analyzed and counted the backward trajectory during the sampling period;  
 461 several typical types were presented in Fig. S1. Figure S1 (a) shows the type of  
 462 backward trajectory with the highest frequency during the sample collection in BJ.  
 463 This type of long-distance transportation from the northwest accounted for  
 464 approximately 43.9% of all cases. The average  $PM_{2.5}$  concentration, carbonaceous  
 465 aerosol concentration, and  $f_{nf}$  of the sample were  $45.4 \pm 22.7 \mu\text{g m}^{-3}$ ,  $9.5 \pm 6.4 \mu\text{gC}$

466  $\text{m}^{-3}$ , and  $56 \pm 10\%$ , respectively. As shown in Fig. S1 (b), when air mass was  
467 transported from the south or stayed for a long time in the Hebei province, air  
468 pollution was usually more serious. These cases accounted for approximately 26.3%  
469 of all cases. The average concentrations of  $\text{PM}_{2.5}$  and carbonaceous aerosols were  
470  $97.3 \pm 43.6 \mu\text{g m}^{-3}$  and  $15.6 \pm 7.9 \mu\text{gC m}^{-3}$ , which were 2.1 and 1.6 times of those in  
471 the northwest, respectively. The aerosol concentration of air masses transported from  
472 the southern region was higher than that from the northern regions. The  $f_{\text{nf}}$  value in  
473 these cases was  $46 \pm 5\%$ , which was 10% higher than in the northwest cases. Thus, air  
474 pollution in BJ might be affected by fossil sources in the Hebei province and other  
475 southern regions.

476 The  $\text{PM}_{2.5}$  and carbonaceous concentrations were low when the air mass  
477 transported from the northwest for a long distance at the XA site (Fig. S1 (c)). In this  
478 case, the average  $\text{PM}_{2.5}$  concentration, carbonaceous aerosol concentration, and  $f_{\text{nf}}$  of  
479 the samples were  $93.1 \pm 65.1 \mu\text{g m}^{-3}$ ,  $17.4 \pm 9.6 \mu\text{gC m}^{-3}$ , and  $62 \pm 7\%$ , respectively.  
480 However, when air masses circulated in the Guanzhong Basin or converged into the  
481 basin from multiple directions due to the local topography (Fig. S1 (d)), the  
482 concentration of carbonaceous aerosol was usually high. The proportion of this type  
483 of air mass transportation accounted for 53.6% of the total cases. The average  $\text{PM}_{2.5}$   
484 concentration, carbonaceous aerosol concentration, and  $f_{\text{nf}}$  of the corresponding  
485 samples were  $132.0 \pm 72.8 \mu\text{g m}^{-3}$ ,  $19.7 \pm 10.4 \mu\text{gC m}^{-3}$ , and  $58 \pm 9\%$ , respectively.  
486 Thus, air pollution in XA was mainly affected by the diffusion environment. The air  
487 mass remained in the upper part of the Guanzhong region for a long time when the  
488 diffusion environment was poor, causing secondary reactions and air pollution.  
489 Moreover, when the air mass came from eastern cities (e.g., Henan or Hubei  
490 provinces),  $f_{\text{nf}}$  was 47%, which was significantly lower than that in other cases. This

491 indicated that fossil source emissions in Henan and other eastern regions might  
492 contribute to air pollution in XA.

493 As shown in Fig. S1 (e), when the air mass was long-distance transported to the  
494 LF, the concentration of carbonaceous aerosols was relatively stable. However,  
495 pollutants accumulated when the air mass returned over and around the city (Fig. S1  
496 (f)). In these cases, the concentrations of  $PM_{2.5}$  and carbonaceous aerosols of the  
497 sample increased by 46.35–57.10%, and  $f_{\text{hf}}$  decreased by 5%. Thus, the LF samples  
498 were more susceptible to the diffusion environment and the proportion of fossil  
499 sources discharged locally.

500 Air pollution in BJ was more susceptible to the impact of transportation from the  
501 southern region, whereas XA and LF were more affected by local emissions and  
502 diffusion environments.

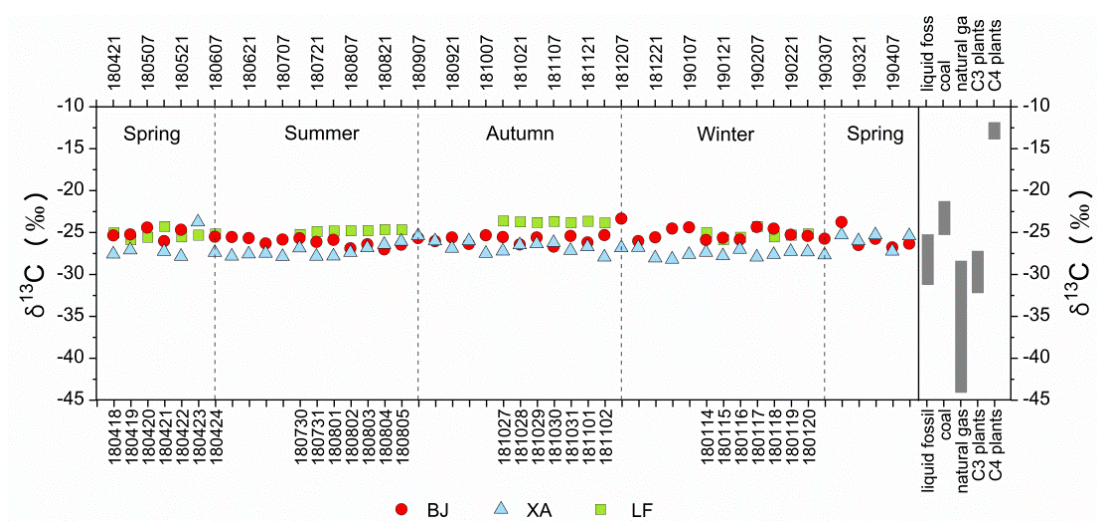
503

#### 504 **3.4 Best estimate of source apportionment of TC using $^{14}\text{C}$ and $^{13}\text{C}$**

505 The  $\delta^{13}\text{C}$  values at the sampling sites in BJ, XA, and LF were  $-25.65 \pm 0.79\text{‰}$ ,  
506  $-26.94 \pm 0.92\text{‰}$ , and  $-23.84 \pm 0.16\text{‰}$ , respectively. Figure 6 shows the  $\delta^{13}\text{C}$  values  
507 of the samples from each city and various sources. Specifically,  $\delta^{13}\text{C}$  had lower values  
508 in the BJ and LF samples during summer ( $-26.11 \pm 0.49\text{‰}$  and  $-24.88 \pm 0.18\text{‰}$ ,  
509 respectively) and higher values during winter ( $-25.07 \pm 0.79\text{‰}$  and  $-23.84 \pm 0.16\text{‰}$ ,  
510 respectively). Conversely, the lower and higher  $\delta^{13}\text{C}$  values in the XA samples  
511 appeared in winter ( $-27.49 \pm 0.44\text{‰}$ ) and spring ( $-26.34 \pm 1.23\text{‰}$ ).

512 Compared with the existing isotope indicators of various sources (Fig. 6), the  
513 increase in  $\delta^{13}\text{C}$  in the BJ and LF samples during winter may be more related to the  
514 increase in coal combustion from local and the surrounding cities. The increase in  
515  $\delta^{13}\text{C}$  in XA samples during autumn and winter may be related to the use of C4 plant

516 fuel, whereas the decrease during winter may be related to vehicle emissions and the  
 517 use of C3 plant fuels, such as wheat straw or wood.



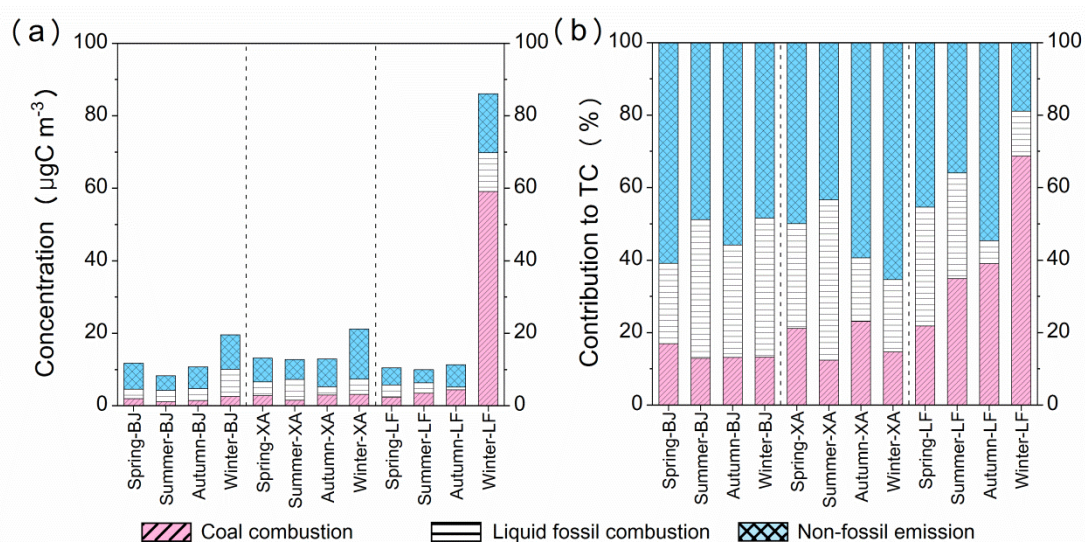
518

519 Fig. 6  $\delta^{13}\text{C}$  values of samples from Beijing (BJ), Xi'an (XA), and Linfen (LF), and  
 520 comparison with the  $\delta^{13}\text{C}$  distribution of various sources. The abscissa represents the  
 521 sampling date (yymmdd). The tick labels of top axis represent the date of BJ and XA,  
 522 and the bottom represents the date of LF. The gray box indicates the  $\delta^{13}\text{C}$  of the main  
 523 source (Agnihotri et al., 2011; Huang et al., 2006; Lopez-Veneroni, 2009; Martinelli  
 524 et al., 2002; Moura et al., 2008; Pugliese et al., 2017; Smith & Epstein, 1971; Vardag  
 525 et al., 2015; Widory, 2006).

526  $^{14}\text{C}$  and  $^{13}\text{C}$  were used to quantify the sources of TC in the carbonaceous aerosols  
 527 (Fig. 7). For the carbonaceous aerosols in BJ and XA, the best estimate of source  
 528 apportionment showed that the contributions of liquid fossil fuels were  $29.3 \pm 12.7\%$   
 529 and  $24.9 \pm 18.0\%$ , respectively, which were greater than the contribution of coal ( $15.5$   
 530  $\pm 8.8\%$  and  $20.9 \pm 14.2\%$ , respectively). In 2019, coal accounted for only 2.6% of all  
 531 fossil fuels used in BJ (BJMBS, 2020). This indicates that the local combustion of  
 532 coal was very low, and the coal contribution might be somewhat related to  
 533 transportation from the surrounding regions. Moreover, the higher contribution of  
 534 liquid fossil fuels in BJ was due to the high number of motor vehicles (6.4 million),



535 which was 1.7 times higher than that in XA in 2019(BJMBS, 2020; XAMBS, 2020).  
 536 Figure S2 shows some studies on the source apportionment of coal and liquid fossil  
 537 fuels in aerosols in BJ over the past few decades. The coal contribution in BJ  
 538 decreased, whereas liquid fossil fuels gradually became the main source of fossil fuels.  
 539 After the implementation of the Action Plan, the proportion of coal in fossil sources  
 540 decreased by approximately 32% in BJ (Gao et al., 2018; Li et al., 2013; Liu et al.,  
 541 2014; Shang et al., 2019; Song et al., 2006; Tian et al., 2016; Wang et al., 2008;  
 542 Zhang et al., 2014).



543  
 544 Fig. 7 Mass concentrations ( $\mu\text{gC m}^{-3}$ ) (a) and percentage (b) of coal combustion,  
 545 liquid fossil fuel, and non-fossil sources emissions for carbonaceous aerosols samples  
 546 in Beijing (BJ), Xi'an (XA), and Linfen (LF) during different seasons.

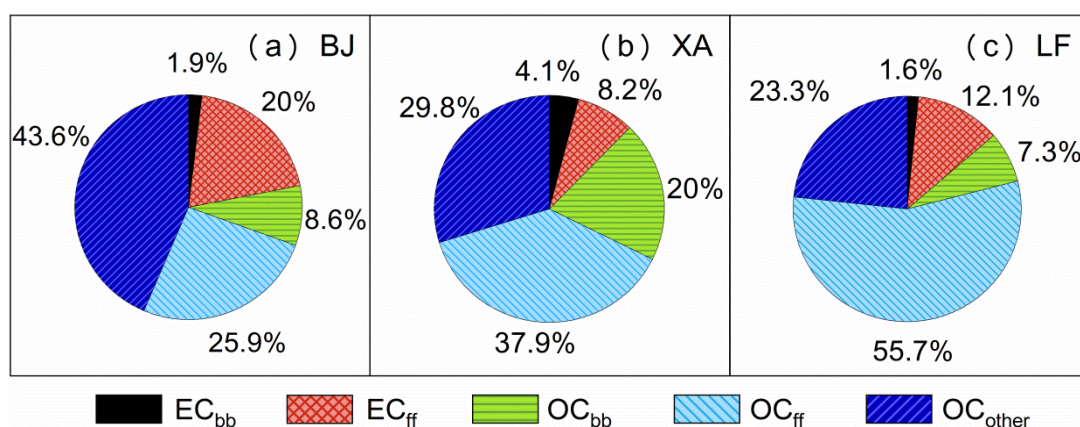
547 In contrast, coal combustion contributed  $42.9 \pm 19.4\%$  to LF samples, which was  
 548 greater than the contribution of liquid fossil emissions ( $20.9 \pm 12.3\%$ ) and  
 549 significantly higher than those in BJ and XA. Especially in winter, coal contributed as  
 550 much as  $68.6 \pm 3.6\%$  ( $59.1 \pm 10.0 \mu\text{gC m}^{-3}$ ). According to the data released by the  
 551 Shanxi Provincial Bureau of Statistics, coal consumption in Shanxi Province was as  
 552 high as 349.06 million tons in 2019, which was 46.7 times of the consumption of

553 liquid fossil fuels, accounting for 70.3% of the total fossil fuel consumption (SPBS,  
 554 2020). The high contribution of coal combustion in winter might be related to the use  
 555 of household coal for heating by rural residents in Shanxi. This is because household  
 556 coal can emit a large amount of carbonaceous particles and is an important source of  
 557 carbonaceous aerosols in rural areas in northern China (Chen et al., 2005; Shen et al.,  
 558 2010; Streets et al., 2003a; Zhi et al., 2008).

559

### 560 3.5 Best estimate of source apportionment of OC and EC by $^{14}\text{C}$ and Lev

561 The concentration of each carbon component in BJ, XA, and LF was calculated  
 562 based on the combination of Lev and  $^{14}\text{C}$ . The best estimate of source apportionment  
 563 showed in Fig. 8. The contributions of  $\text{OC}_{\text{other}}$  ( $43.6 \pm 12.9\%$ ),  $\text{OC}_{\text{ff}}$  ( $25.5 \pm 11.7\%$ ),  
 564 and  $\text{EC}_{\text{ff}}$  ( $20.5 \pm 6.5\%$ ) were relatively high in BJ. The  $\text{OC}_{\text{bb}}$  ( $23.0 \pm 17.3\%$ ) and  $\text{OC}_{\text{ff}}$   
 565 ( $39.7 \pm 9.7\%$ ) were the highest contributors in XA. The LF samples showed different  
 566 characteristics, and the contribution of fossil sources was significantly high, especially  
 567 for the  $\text{OC}_{\text{ff}}$  ( $56.1 \pm 11.9\%$ ).

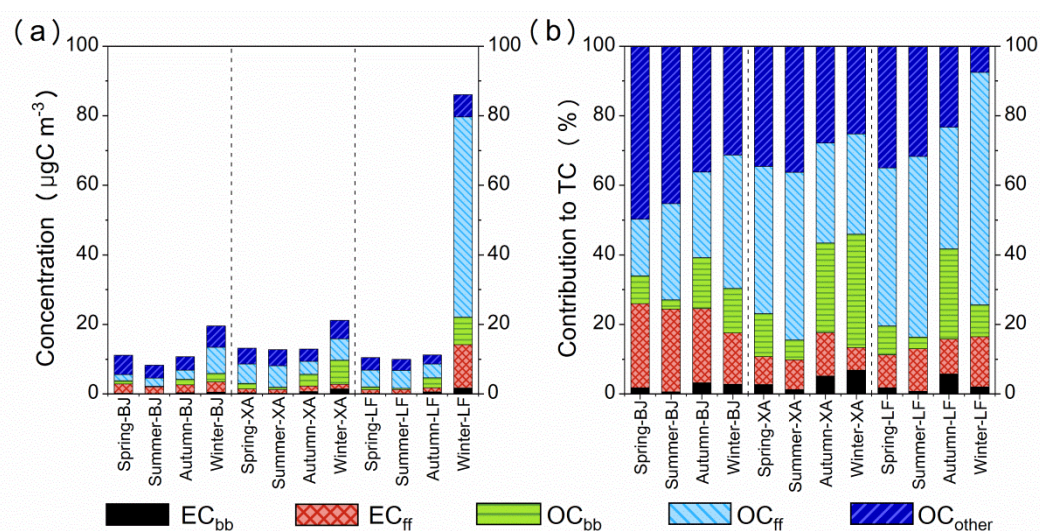


568

569 Fig. 8 Percentage of elemental carbon from biomass burning ( $\text{EC}_{\text{bb}}$ ) and fossil-fuel  
 570 combustion ( $\text{EC}_{\text{ff}}$ ) and percentage of organic carbon from biomass burning ( $\text{OC}_{\text{bb}}$ ),  
 571 fossil-fuel combustion ( $\text{OC}_{\text{ff}}$ ), and other sources ( $\text{OC}_{\text{other}}$ ) for the  $\text{PM}_{2.5}$  samples in  
 572 Beijing (BJ), Xi'an (XA), and Linfen (LF).

### 573 3.5.1 Biomass burning contribution to TC

574 The concentrations ( $0.3 \pm 0.3 \mu\text{gC m}^{-3}$ ) and contributions ( $1.9 \pm 1.4\%$ ) of  $\text{EC}_{\text{bb}}$  in  
 575 BJ were relatively low during the whole year (Fig. 9). The  $\text{EC}_{\text{bb}}$  at the XA and LF  
 576 sites had high concentrations in autumn ( $0.7 \pm 0.5 \mu\text{gC m}^{-3}$  and  $0.6 \pm 0.1 \mu\text{gC m}^{-3}$ ) and  
 577 winter ( $1.5 \pm 0.7 \mu\text{gC m}^{-3}$  and  $1.7 \pm 0.3 \mu\text{gC m}^{-3}$ ) and low concentrations in summer  
 578 ( $0.2 \pm 0.1 \mu\text{gC m}^{-3}$  and  $0.1 \pm 0.0 \mu\text{gC m}^{-3}$ ), respectively.



579

580 Fig. 9 Mass concentrations ( $\mu\text{gC m}^{-3}$ ) (a) and percentage (b) of elemental carbon from  
 581 biomass burning ( $\text{EC}_{\text{bb}}$ ) and fossil-fuel combustion ( $\text{EC}_{\text{ff}}$ ), organic carbon from  
 582 biomass burning ( $\text{OC}_{\text{bb}}$ ), fossil-fuel combustion ( $\text{OC}_{\text{ff}}$ ), and other sources ( $\text{OC}_{\text{other}}$ ) for  
 583 carbonaceous aerosols samples in Beijing (BJ), Xi'an (XA), and Linfen (LF) during  
 584 different seasons.

585 The  $\text{OC}_{\text{bb}}$  concentrations in the BJ, XA, and LF samples showed an increase in  
 586 autumn ( $1.6 \pm 1.4 \mu\text{gC m}^{-3}$ ,  $3.3 \pm 2.2 \mu\text{gC m}^{-3}$ , and  $2.9 \pm 0.4 \mu\text{gC m}^{-3}$ ) and winter ( $2.5$   
 587  $\pm 2.1 \mu\text{gC m}^{-3}$ ,  $6.9 \pm 3.3 \mu\text{gC m}^{-3}$ , and  $7.9 \pm 1.3 \mu\text{gC m}^{-3}$ ), respectively. Especially in  
 588 the XA samples,  $\text{OC}_{\text{bb}}$  had high contributions in autumn ( $28.6 \pm 15.8\%$ ) and winter  
 589 ( $32.8 \pm 12.3\%$ ). The contribution of biomass combustion in XA ( $24.1 \pm 18.0\%$ ) was  
 590 significantly larger than that in BJ ( $10.8 \pm 7.9\%$ ) and LF ( $8.8 \pm 8.9\%$ ), which was also  
 591 reflected in the concentration of Lev (Fig. S3). The Lev concentration in XA ( $0.36 \pm$

592  $0.38 \mu\text{g m}^{-3}$ ) was higher than that in BJ ( $0.15 \pm 0.17 \mu\text{g m}^{-3}$ ) and slightly higher than  
593 that in LF ( $0.32 \pm 0.34 \mu\text{g m}^{-3}$ ). Furthermore, the Lev concentration in XA during  
594 autumn and winter was up to 5.3 times higher than that during the other seasons.  
595 Especially in winter, the proportion of Lev in the TC was  $4.0 \pm 2.3\%$  in XA, which  
596 was 3.9 and 3.8 times those in BJ and LF, respectively.

597 Zhang et al. (2015) attributed this to emissions from neighboring rural regions  
598 because such areas use biofuels for heating and cooking more commonly in winter.  
599 China produces 939 million tons of agricultural biomass residues annually, which is  
600 the main energy source for some rural areas (Liao et al., 2004; Lu et al., 2009). In  
601 addition, the increase in urban vegetation coverage may also increase the  
602 photochemical reactions of biological volatile organic compounds (VOCs) (Gelencsér  
603 et al., 2007; NBS, 2021). Therefore, in recent years, non-fossil fuels have gradually  
604 become a major contributor to carbonaceous aerosols in BJ and XA with the reduction  
605 in the use of fossil energy.

### 606 **3.5.2 Fossil contribution to TC**

607 The  $\text{EC}_{\text{ff}}$  concentrations at BJ (spring:  $2.7 \pm 1.4 \mu\text{gC m}^{-3}$ ; summer:  $2.0 \pm 0.8 \mu\text{gC}$   
608  $\text{m}^{-3}$ ; autumn:  $2.3 \pm 2.0 \mu\text{gC m}^{-3}$ ; winter:  $2.9 \pm 2.6 \mu\text{gC m}^{-3}$ ) and XA (spring:  $1.1 \pm 0.8$   
609  $\mu\text{gC m}^{-3}$ ; summer:  $1.1 \pm 1.1 \mu\text{gC m}^{-3}$ ; autumn:  $1.6 \pm 2.3 \mu\text{gC m}^{-3}$ ; winter:  $1.4 \pm 0.8$   
610  $\mu\text{gC m}^{-3}$ ) did not fluctuate significantly during the year. The concentration of  $\text{EC}_{\text{ff}}$  in  
611 LF during spring, summer, and autumn was relatively stable ( $1.0\text{--}1.2 \mu\text{gC m}^{-3}$ ), but it  
612 was high during winter ( $12.5 \pm 2.5 \mu\text{gC m}^{-3}$ ), reaching 10.2 times that in summer.

613 The concentration of  $\text{OC}_{\text{ff}}$  was slightly higher in XA during summer ( $6.2 \pm 2.2$   
614  $\mu\text{gC m}^{-3}$ ) and winter ( $6.1 \pm 2.1 \mu\text{gC m}^{-3}$ ). The contribution of  $\text{OC}_{\text{ff}}$  in the BJ samples  
615 increased to  $32.4 \pm 14.5\%$  during winter and decreased to  $18.4 \pm 8.4\%$  during spring.  
616 The  $\text{OC}_{\text{ff}}/\text{EC}_{\text{ff}}$  ratios in BJ and LF during winter were approximately  $2.3 \pm 1.2$  and 4.7

617  $\pm 0.7$ , respectively, suggesting that the fossil source secondary carbonaceous aerosols  
618 were higher in winter. This can be explained by the lower temperature in the winter  
619 altering the gas–particle equilibrium, suggesting that a larger portion of the  $OC_{ff}$   
620 during winter was secondary aerosol (Genberg et al., 2011).  $OC_{ff}$  in LF had high  
621 concentrations in winter ( $57.6 \pm 9.2 \mu\text{gC m}^{-3}$ ) and low concentrations in summer ( $5.2$   
622  $\pm 1.2 \mu\text{gC m}^{-3}$ ). This indicated that the burning of fossil sources was an important  
623 source of OC in BJ ( $OC_{ff}$ :  $32.4 \pm 14.5\%$ ) and LF ( $OC_{ff}$ :  $66.8 \pm 1.7\%$ ) during winter.  
624 Fang et al. (2017) found that fossil fuels contributed significantly ( $> 50\%$ ) to carbon  
625 components in the haze in East Asia during January 2014, suggesting that the aerosol  
626 contribution was generally dominated by fossil combustion sources. Therefore, using  
627 cleaner energy and cleaner residential stoves to reduce and replace the high-emission  
628 end-use coal combustion processes and control the emissions from liquid-fossil-fueled  
629 vehicles in megacities should be beneficial to the air quality.

### 630 **3.5.3 Other non-fossil contributions to OC**

631 In addition to the OC directly emitted from fossil and biomass fuels, there are  
632 many components of OC, such as SOC, whose source is difficult to identify.  
633 Residential oil fume emissions from urban residents, emissions from biological  
634 sources, and secondary bio-organic aerosols generated by the secondary reaction of  
635 biomass fuels are also important components of OC (Gelencsér et al., 2007; Zhang et  
636 al., 2015).

637 The concentration of  $OC_{other}$  in the LF samples did not vary greatly during spring  
638 ( $3.7 \pm 1.2 \mu\text{gC m}^{-3}$ ) and summer ( $3.2 \pm 0.5 \mu\text{gC m}^{-3}$ ) but it was lower in autumn ( $2.6 \pm$   
639  $0.3 \mu\text{gC m}^{-3}$ ) and higher in winter ( $6.5 \pm 2.8 \mu\text{gC m}^{-3}$ ). In BJ, the contribution of  
640  $OC_{other}$  was high during spring ( $49.9 \pm 9.9\%$ ) and summer ( $45.8 \pm 9.8\%$ ), and its  
641 concentration was relatively high during winter ( $6.1 \pm 5.6 \mu\text{gC m}^{-3}$ ). Zhang et al.

642 (2015) mainly attributed the presence of OC<sub>other</sub> in northern China to SOC formation  
643 from non-fossil, non-biogenic precursors. In general, secondary bio-organic aerosols  
644 in spring and autumn are mainly caused by biological emissions or long-distance  
645 transportation of biological VOCs and secondary organic aerosols (SOAs) in  
646 particulates (Gelencsér et al., 2007; Jimenez et al., 2009). The high concentration in  
647 winter may be because low temperatures drive condensable semi-volatile organic  
648 compounds (SVOCs) into the particulate phase (Simpson et al., 2007; Tanarit et al.,  
649 2008).

650 The OC<sub>other</sub> contribution and concentration in XA were high in summer ( $35.2 \pm$   
651  $10.0\%$ ) and winter ( $5.4 \pm 4.2 \mu\text{gC m}^{-3}$ ), respectively. We assume that this excess is  
652 mainly attributed to SOC formation from non-fossil and primary biogenic particles.  
653 Some SOAs are formed by VOCs that are produced by burning wood or biofuels (e.g.,  
654 ethanol), and they increase the load of these sources on organic aerosols (Genberg et  
655 al., 2011). Huang et al. (2014) found that severe haze pollution was largely driven by  
656 secondary aerosol formation, and non-fossil SOAs dominated, accounting for  $66 \pm 8\%$   
657 of the SOAs in XA despite extensive urban emissions. Ni et al. (2020) also considered  
658 that non-fossil sources largely contributed (56%) to SOC in XA. Thus, the control of  
659 biomass burning activities could be an efficient strategy for reducing aerosols,  
660 especially in XA. Furthermore, SOC formation from these non-fossil VOCs may be  
661 enhanced when they are mixed with other pollutants, such as VOCs and NO<sub>x</sub> (Hoyle  
662 et al., 2011; Weber et al., 2007). Motor vehicles are one of the main anthropogenic  
663 sources of VOCs and NO<sub>x</sub> (Barletta et al., 2005; Liu et al., 2008). In Section 3.4, we  
664 found that the carbonaceous concentrations from motor vehicle emissions were high  
665 in XA during winter and summer (Fig. 7a), and the increasing of motor vehicle  
666 activities might partly explain the high concentration of OC<sub>other</sub> during the two

667 seasons.

668

### 669 **3.6 Uncertainty analysis**

670 The results of the uncertainty analysis of the given set (Table 1) of the  
671 parameters in the three cities were shown in Fig. 10. Each curve represents the  
672 probability distribution of the sources of carbon components that contribute to the TC,  
673 from which the uncertainty of the source allocation can be derived. Some results were  
674 uncertain because the input parameters of the LHS calculation varied greatly. The  
675 contributions of  $OC_{ff}$  and  $OC_{other}$  to the TC were mostly uncertain. This is mainly  
676 related to the uncertainty of the two parameters,  $Lev/OC_{bb}$  and  $(EC/OC)_{bb}$ . Both these  
677 parameters depend on the burning conditions and type of biomass, as mentioned in  
678 Section 2.9. More reliable data would be obtained if  $^{13}C/^{14}C$  could be performed on  
679 the pure OC fractions of the samples, which has been proven to be feasible (Huang et  
680 al., 2014; Szidat et al., 2004, 2006; Zhang et al., 2015). Other contributions have  
681 single peaks, which prove that the results of the source analysis are reliable. These  
682 results demonstrate that we can identify the main contributors.



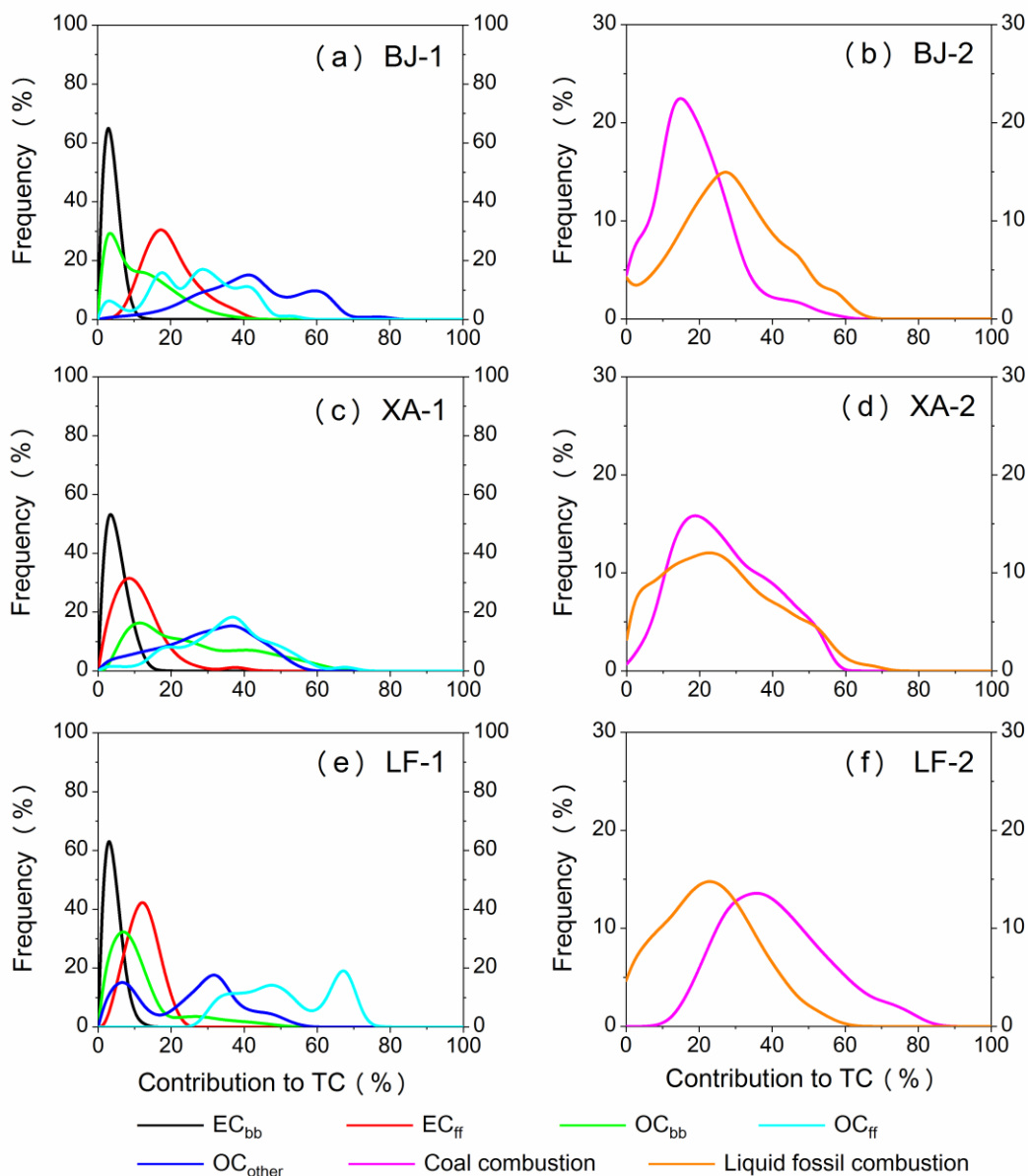


Fig. 10 Latin hypercube sampling of frequency distributions of the source contributions to total carbon (TC) from fossil, organic carbon (OC), and elemental carbon (EC) source categories (Table 1) for the samples collected in Beijing (BJ), Xi'an (XA), and Linfen (LF).

## 4 Conclusions

PM<sub>2.5</sub> samples were collected from BJ, XA, and LF in northern China from January 2018 to April 2019. The main objective of this study was to quantify the



692 sources of carbonaceous aerosols by measuring the EC, OC, Lev,  $^{13}\text{C}$ , and  $^{14}\text{C}$   
693 combined with LHS.

694 The TC accounted for approximately  $17.5 \pm 6\%$ ,  $21.5 \pm 21\%$ , and  $17.8 \pm 7.2\%$  of  
695  $\text{PM}_{2.5}$  in the samples from BJ, XA, and LF, and the corresponding concentrations  
696 were  $12.5 \pm 11.8 \mu\text{gC m}^{-3}$ ,  $14.6 \pm 7.5 \mu\text{gC m}^{-3}$ , and  $35.7 \pm 36.5 \mu\text{gC m}^{-3}$ , respectively.  
697 The concentrations at the three sites showed high values in winter and low values in  
698 summer. Based on backward trajectory analysis, we found that carbonaceous aerosols  
699 in BJ were more susceptible to transportation from the southern regions. Local  
700 emissions and the diffusion environment significantly impacted carbonaceous  
701 aerosols in XA and LF.

702 The best estimate of source apportionment of the fossil components in the TC  
703 showed that the contribution of liquid fossil fuel combustion was  $29.3 \pm 12.7\%$  and  
704  $24.9 \pm 18.0\%$  in BJ and XA, respectively, which was greater than the contribution of  
705 coal combustion ( $15.5 \pm 8.8\%$ ;  $20.9 \pm 14.5\%$ ). In contrast, coal combustion  
706 contributed  $42.9 \pm 19.4\%$  in LF, which was greater than the contribution of liquid  
707 fossil fuel combustion ( $20.9 \pm 12.3\%$ ).

708 The best estimate of source apportionment of OC and EC indicated that the  
709 contributions of  $\text{EC}_{\text{ff}}$  ( $20.0 \pm 6.5\%$ ),  $\text{OC}_{\text{ff}}$  ( $25.9 \pm 11.6\%$ ), and  $\text{OC}_{\text{other}}$  ( $43.6 \pm 12.9\%$ )  
710 were relatively high in BJ. The  $\text{OC}_{\text{ff}}$  contribution was higher in winter ( $32.4 \pm 14.5\%$ ),  
711 and its concentration was 3.3 times higher than that in other seasons. The contribution  
712 of  $\text{OC}_{\text{bb}}$  ( $20.0 \pm 15.3\%$ ) and  $\text{OC}_{\text{ff}}$  ( $37.9 \pm 10.8\%$ ) was higher in XA. The contribution  
713 of biomass burning to the TC was as high as  $39.6 \pm 14.5\%$  in winter. The contribution  
714 of  $\text{OC}_{\text{ff}}$  in LF was significantly high ( $55.7 \pm 12.2\%$ ), especially in winter ( $66.8 \pm$   
715  $1.7\%$ ).

716 The decline (6–16%) in the contribution of fossil sources since the

717 implementation of the Action Plan indicates the effectiveness of air quality  
718 management. In the future, the government needs to further regulate and control  
719 emissions from motor vehicles in megacities such as BJ and XA. The cleaner use of  
720 coal must be further strengthened in coal-based cities such as LF in the eastern part of  
721 the Fenwei Plain. This study indicates that attention should be paid to the control of  
722 biomass burning in northern China, especially in the Guanzhong region.

723

724 ***Code and data availability:*** The data products in this paper are available at the East  
725 Asian Paleoenvironmental Science Database, National Earth System Science Data  
726 Center, National Science & Technology Infrastructure of China  
727 ([http://paleodata.ieecas.cn/index\\_EN.aspx](http://paleodata.ieecas.cn/index_EN.aspx)).

728

729 ***Author contributions:*** HZ performed the data analysis and wrote the initial draft of  
730 the manuscript. ZN and WZ conceived the project and reviewed the paper. ZN and  
731 SW provided the samples. HZ, XF, SW, XL and HD conducted the measurements. All  
732 authors made substantial contributions to this work.

733

734 ***Competing interests:*** The authors declare that they have no conflict of interest.

735

736 ***Acknowledgments:*** The authors acknowledge the help of anonymous reviewers for  
737 improving this article.

738

739 ***Financial support:*** The study was financially supported by the Strategic Priority  
740 Research Program of the Chinese Academy of Sciences (XDA23010302), National  
741 Research Program for Key Issues in Air Pollution Control (DQGG0105-02), the

742 National Natural Science Foundation of China (41730108, 42173082, and 41773141),  
743 Natural Science Foundation of Shaanxi province (2014JQ2-4018), Key projects of  
744 CAS (ZDRW-ZS-2017-6), and Natural Science Basic Research Program of Shaanxi  
745 Province (2019JCW-20).

746

#### 747 *References*

748 Aggarwal, S. G., and Kawamura, K.: Molecular distributions and stable carbon  
749 isotopic compositions of dicarboxylic acids and related compounds in aerosols  
750 from Sapporo, Japan: Implications for photochemical aging during long-range  
751 atmospheric transport, *J. Geophys. Res.*, 113, D14301,  
752 <https://doi.org/10.1029/2007JD009365>, 2008.

753 Agnihotri, R., Mandal, T. K., Karapurkar, S. G., Naja, M., Gadi, R., Ahammed, Y.  
754 N., Kumar, A., Saud, T., and Saxena, M.: Stable carbon and nitrogen isotopic  
755 composition of bulk aerosols over India and northern Indian Ocean, *Atmos.*  
756 *Environ.*, 45, 2828-2835, <https://doi.org/10.1016/j.atmosenv.2011.03.003>, 2011.

757 Andersson, A., Deng, J. J., Du, K., Zheng, M., Yan, C. Q., Sköld, M., and Gustafsson,  
758 O. r.: Regionally-varying combustion sources of the January 2013 severe haze  
759 events over eastern China, *Environ. Sci. Technol.*, 49, 2038-2043,  
760 <https://doi.org/10.1021/es503855e>, 2015.

761 Bachar, A., Markus-Shi, J., Regev, L., Boaretto, E., and T. Klein, T.: Tree rings reveal  
762 the adverse effect of water pumping on protected riparian *Platanus orientalis* tree  
763 growth, *For. Ecol. Manag.*, 458, 0378-1127,  
764 <https://doi.org/10.1016/j.foreco.2019.117784>, 2020.

765 Barletta, B., Meinardi, S., Rowland, F. S., Chan, C., Wang, X. M., Zou, S. C., Chan,  
766 L., and Blake, D. R.: Volatile organic compounds in 43 Chinese cities, *Atmos.*

767 Environ., 39, 5979-5990, <https://doi.org/10.1016/j.atmosenv.2005.06.029>, 2005.

768 BJMBS: (Beijing Municipal Bureau Statistics): Beijing Statistical Yearbook-2020,  
769 China Statistics press.,  
770 <http://nj.tjj.beijing.gov.cn/nj/main/2020-tjnj/zk/indexch.htm>, 2020 (last access:  
771 28 March 2022).

772 Cachier, H., Buat Menard, P., Fontugne, M., and Rancher, J.: Source terms and source  
773 strengths of the carbonaceous aerosol in the tropics, *J. Atmos. Chem.*, 3, 469-489,  
774 <https://doi.org/10.1007/BF00053872>, 1985.

775 Cachier, H., Buat Menard, P., Fontugne, M., and Chesselet, R.: Long - range transport  
776 of continentally-derived particulate carbon in the marine atmosphere: Evidence  
777 from stable carbon isotope studies, *Tellus B*, 38, 161-177,  
778 <https://doi.org/10.1111/j.1600-0889.1986.tb00184.x>, 1986.

779 Cao, J. J., Lee, S. C., Ho, K. F., Zhang, X. Y., Zou, S. C., Fung, K., Chow, J. C., and  
780 Watson, J. G.: Characteristics of carbonaceous aerosol in Pearl River Delta  
781 Region, China during 2001 winter period, *Atmos. Environ.*, 37, 1451-1460,  
782 [https://doi.org/10.1016/S1352-2310\(02\)01002-6](https://doi.org/10.1016/S1352-2310(02)01002-6), 2003.

783 Cao, J. J., Lee, S. C., Chow, J. C., Watson, J. G., Ho, K. F., Zhang, R. J., Jin, Z. D.,  
784 Shen, Z. X., Chen, G. C., and Kang, Y. M.: Spatial and seasonal distributions of  
785 carbonaceous aerosols over China, *Journal of Geophysical Research*  
786 *Atmospheres*, D112, 22-11, <https://doi.org/10.1029/2006JD008205>, 2007.

787 Cao, J. J., Zhu, C. S., Chow, J. C., Watson, J. G., Han, Y. M., Wang, G. H., Shen, Z. X.,  
788 and An, Z. S.: Black carbon relationships with emissions and meteorology in  
789 Xi'an, China, *Atmos. Res.*, 94, 194-202, <https://doi.org/10.1029/2006JD008205>,  
790 2009.

791 Cao, J. J., Chow, J. C., Tao, J., Lee, S. C., Watson, J. G., Ho, K., Wang, G. H., Zhu, C.

792 S., and Han, Y. M.: Stable carbon isotopes in aerosols from Chinese cities:  
793 Influence of fossil fuels, *Atmos. Environ.*,  
794 <https://doi.org/10.1016/j.atmosenv.2010.10.056>, 2011.

795 Cao, J. J., Shen, Z. X., Chow, J. C., Watson, J. G., Lee, S. C., Tie, X. X., Ho, K. F.,  
796 Wang, G. H., and Han, Y. M.: Winter and summer PM<sub>2.5</sub> chemical compositions  
797 in fourteen Chinese Cities, *Air Waste Manage Assoc*, 62, 1214–1226,  
798 <https://doi.org/10.1080/10962247.2012.701193>, 2012.

799 Castro, L. M., Pio, C. A., Harrison, R. M., and Smith, D.: Carbonaceous aerosol in  
800 urban and rural European atmospheres: estimation of secondary organic carbon  
801 concentrations, *Atmos. Environ.*, 33, 2771–2781,  
802 <https://doi.org/10.1111/j.1553-2712.2005.tb00860.x>, 1999.

803 Ceburnis, D., Garbaras, A., Szidat, S., Rinaldi, M., Fahrni, S., Perron, N., Wacker, L.,  
804 Leinert, S., Remeikis, V., Facchini, M. C., Prevot, A. S. H., Jennings, S. G., and  
805 O’Dowd, C. D.: Quantification of the carbonaceous matter origin in submicron  
806 marine aerosol particles by dual carbon isotope analysis, *Atmos. Chem. Phys.*  
807 *Discuss.*, 11, 8593–8606, <https://doi.org/10.5194/acpd-11-2749-2011>, 2011.

808 Chen, Y. J., Sheng, G. Y., Bi, X. H., Feng, Y. L., Mai, B. X., and Fu, J. M.: Emission  
809 Factors for Carbonaceous Particles and Polycyclic Aromatic Hydrocarbons from  
810 Residential Coal Combustion in China, *Environ. Sci. Technol.*, 39, 1861–1867,  
811 <https://doi.org/10.1021/es0493650>, 2005.

812 Chesselet, R., Fontugne, M., Buat Menard, P., Ezat, U., and Lambert, C. E.: The  
813 origin of particulate organic carbon in the marine atmosphere as indicated by its  
814 stable carbon isotopic composition, *Geophys. Res. Lett.*, 8, 345–348,  
815 <https://doi.org/10.1029/GL008i004p00345>, 1981.

816 Chow, J. C., and Watson, J. G.: PM<sub>2.5</sub> carbonate concentrations at regionally

817 representative Interagency Monitoring of Protected Visual Environment sites,  
818 Journal of Geophysical Research Atmospheres, 107,  
819 <https://doi.org/10.1029/2001JD000574>, 2002.

820 Chow, J. C., Watson, J. G., Chen, L. W. A., Arnott, W. P., Moosmüller, H., and Fung,  
821 K.: Equivalence of Elemental Carbon by Thermal/Optical Reflectance and  
822 Transmittance with Different Temperature Protocols, Environ. Sci. Technol., 38,  
823 4414-4422, <https://doi.org/10.1021/es034936u>, 2004.

824 Claeys, M., Kourchev, I., Pashynska, V., Vas, G., Vermeylen, R., Wang, W., Cafmeyer,  
825 J., Chi, X., Artaxo, P., Andreae, M. O., and Maenhaut, W.: Polar organic marker  
826 compounds in atmospheric aerosols during the LBA-SMOCC 2002 biomass  
827 burning experiment in Rondônia, Brazil: sources and source processes, time  
828 series, diel variations and size distributions, Atmos. Chem. Phys.,  
829 <https://doi.org/10.5194/acp-10-9319-2010>, 2010.

830 Clarke, A. G., and Karani, G. N.: Characterisation of the carbonate content of  
831 atmospheric aerosols, J. Atmos. Chem., 14, 119-128,  
832 <https://doi.org/10.1007/BF00115228>, 1992.

833 Clayton, G. D., Arnold, J. R., and Patty, F. A.: Determination of Sources of Particulate  
834 Atmospheric Carbon, Science, 122, 751-753,  
835 <https://doi.org/10.1126/science.122.3173.751>, 1955.

836 Coplen, T. B.: New guidelines for reporting stable hydrogen, carbon, and oxygen  
837 isotope-ratio data, Geochim. Cosmochim. Acta, 60, 3359-3360,  
838 [https://doi.org/10.1016/0016-7037\(96\)00263-3](https://doi.org/10.1016/0016-7037(96)00263-3), 1996.

839 CSC: (Chinese State Council): Action Plan for Air Pollution Prevention and Control,  
840 [http://www.gov.cn/zhengce/content/2013-09/13/content\\_4561.htm](http://www.gov.cn/zhengce/content/2013-09/13/content_4561.htm), 2013 (last  
841 access: 28 March 2022).

842 CSC: (Chinese State Council): Three-year action plan to fight air pollution (NO. 2018.  
843 22), [http://www.gov.cn/zhengce/content/2018-07/03/content\\_5303158.htm](http://www.gov.cn/zhengce/content/2018-07/03/content_5303158.htm), 2018  
844 (last access: 28 March 2022).

845 Currie, L. A.: Evolution and Multidisciplinary Frontiers of <sup>14</sup>C Aerosol Science,  
846 *Radiocarbon*, 42, 115-126, <https://doi.org/10.1017/S003382220005308X>, 2000.

847 Draxler, R. R., and Hess, G. D.: An overview of the HYSPLIT\_4 modelling system  
848 for trajectories, dispersion and deposition, *Aust. Meteorol. Mag.*, 47, 295-308,  
849 1998.

850 England, G., Chang, O., and Wien, S.: Development of fine particulate emission  
851 factors and speciation profiles for oil and gas-fired combustion systems, United  
852 States, 2002.

853 Engling, G., Carrico, C. M., Kreidenweis, S. M., Collett Jr., J. L., Day, D. E., Malm, W.  
854 C., Lincoln, E., Hao, W. M., Iinuma, Y., and Herrmann, H.: Determination of  
855 levoglucosan in biomass combustion aerosol by high-performance  
856 anion-exchange chromatography with pulsed amperometric detection, *Atmos.*  
857 *Environ.*, 2006,40, S299-S311, <https://doi.org/10.1016/j.atmosenv.2005.12.069>,  
858 2006.

859 Engling, G., Lee, J. J., Tsai, Y. W., Lung, S. H., C., C., Chou, C. K., and Chan, C.:  
860 Size-Resolved Anhydrosugar Composition in Smoke Aerosol from Controlled  
861 Field Burning of Rice Straw, *Aerosol Sci. Technol.*, 43, 662-672,  
862 <https://doi.org/10.1080/02786820902825113>, 2009.

863 Fang, W., Andersson, A., Zheng, M., Lee, M., Holmstrand, H., Kim, S. W., Du, K.,  
864 and Örjan, G.: Divergent Evolution of Carbonaceous Aerosols during Dispersal  
865 of East Asian Haze, *Sci. Rep.*, 7, 10422,  
866 <https://doi.org/10.1038/s41598-017-10766-4>, 2017.

867 Feng, Y. L., Chen, Y. J., Guo, H., Zhi, G. R., Xiong, S. C., Li, J., Sheng, G. Y., and Fu,  
868 J. M.: Characteristics of organic and elemental carbon in PM<sub>2.5</sub> samples in  
869 Shanghai, China, *Atmos. Res.*, 92, 434-442,  
870 <https://doi.org/10.1016/j.atmosres.2009.01.003>, 2009.

871 Fu, P. Q., Kawamura, K., Chen, J., Li, J., Sun, Y. L., Liu, Y., Tachibana, E., Aggarwal,  
872 S. G., Okuzawa, K., Tanimoto, H., Kanaya, Y., and Wang, Z. F.: Diurnal  
873 variations of organic molecular tracers and stable carbon isotopic composition in  
874 atmospheric aerosols over Mt. Tai in the North China Plain: an influence of  
875 biomass burning, *Atmos. Chem. Phys.*, 12, 8359–8375,  
876 <https://doi.org/10.5194/acp-12-8359-2012>, 2012.

877 Gao, J. J., Wang, K., Wang, Y., Liu, S. H., Zhu, C. Y., Hao, J. M., Liu, H. J., Hua, S.  
878 B., and Tian, H. Z.: Temporal-spatial characteristics and source apportionment of  
879 PM<sub>2.5</sub> as well as its associated chemical species in the Beijing-Tianjin-Hebei  
880 region of China, *Environ. Pollut.*, 233, 714-724,  
881 <https://doi.org/10.1016/j.envpol.2017.10.123>, 2018.

882 Gelencsér, A., May, B., Simpson, D., Sánchez-Ochoa, A., Kasper-Giebl, A., Puxbaum,  
883 H., Caseiro, A., Pio, C., and Legrand, M.: Source apportionment of PM<sub>2.5</sub>  
884 organic aerosol over Europe: Primary/secondary, natural/anthropogenic, and  
885 fossil/biogenic origin, *J. Geophys. Res.: Atmos.*, 112,  
886 <https://doi.org/10.1029/2006jd008094>, 2007.

887 Genberg, J., Hyder, M., Stenström, K., Bergström, R., Simpson, D., Fors, E. O.,  
888 Jönsson, J. A., and Swietlicki, E.: Source apportionment of carbonaceous aerosol  
889 in southern Sweden, *Atmos. Chem. Phys.*, 11, 13575-13616,  
890 <https://doi.org/10.5194/acp-11-11387-2011>, 2011.

891 Guo, J. D., Ge, Y. S., Hao, L. J., Tan, J. W., Li, J. Q., and Feng, X. Y.: On-road



892 measurement of regulated pollutants from diesel and CNG buses with urea  
893 selective catalytic reduction systems, *Atmos. Environ.*,  
894 <https://doi.org/10.1016/j.atmosenv.2014.07.032>, 2014.

895 Hammer, S., and Levin, I.: Monthly mean atmospheric D14CO2 at Jungfrauoch and  
896 Schauinsland from 1986 to 2016, *Tellus B*, 65, 20092,  
897 <https://doi.org/10.11588/data/10100>, 2017.

898 Han, R., Wang, S. X., Shen, W. H., Wang, J. D., Wu, K., Ren, Z. H., and Feng, M. N.:  
899 Spatial and temporal variation of haze in China from 1961 to 2012, *J. Environ.*  
900 *Sci.*, 46, 1001-0742, <https://doi.org/10.1016/j.jes.2015.12.033>, 2016a.

901 Han, Y. M., Chen, L. W., Huang, R. J., Chow, J. C., Watson, J. G., Ni, H. Y., Liu, S. X.,  
902 Fung, K. K., Shen, Z. X., Wei, C., Wang, Q. Y., J. Tian, Zhao, Z. Z., Prévôt, A. S.  
903 H., and Cao, J. J.: Carbonaceous aerosols in megacity Xi'an, China: Implications  
904 of thermal/optical protocols comparison, *Atmos. Environ.*,  
905 <https://doi.org/10.1016/j.atmosenv.2016.02.023>, 2016b.

906 Heal, M. R.: The application of carbon-14 analyses to the source apportionment of  
907 atmospheric carbonaceous particulate matter: a review, *Anal. Bioanal. Chem.*,  
908 406, 81–98, <https://doi.org/10.1007/s00216-013-7404-1>, 2014.

909 Ho, K. F., Lee, S. C., Cao, J. J., Li, Y. S., Chow, J. C., Watson, J. G., and Fung, K.:  
910 Variability of organic and elemental carbon, water soluble organic carbon, and  
911 isotopes in Hong Kong, *Atmos. Chem. Phys.*, 6, 4569–4576,  
912 <https://doi.org/10.5194/acp-6-4569-2006>, 2006.

913 Hoffmann, D., Tilgner, A., Iinuma, Y., and Herrmann, H.: Atmospheric stability of  
914 levoglucosan: a detailed laboratory and modeling study, *Environ. Sci. Technol.*,  
915 44, 694–699, <https://doi.org/10.1021/es902476f>, 2010.

916 Hoyle, C. R., Boy, M., Donahue, N. M., Fry, J. L., Glasius, M., Guenther, A., Hallar,

917 A. G., Hartz, K. H., Petters, M., Petters, T., Rosenoern, T., and Sullivan, A. P.: A  
918 review of the anthropogenic influence on biogenic secondary organic aerosol,  
919 *Atmos. Chem. Phys.*, 11, <https://doi.org/10.5194/acp-11-321-2011>, 2011.

920 Hua, Q., and Barbetti, M.: Review of Tropospheric Bomb <sup>14</sup>C Data for Carbon Cycle  
921 Modeling and Age Calibration Purposes, *Radiocarbon*, 46,  
922 <https://doi.org/10.1017/S0033822200033142>, 2004.

923 Huang, J., Kang, S. C., Shen, C. D., Cong, Z. Y., Liu, K. X., Wang, W., and Liu, L. C.:  
924 Seasonal variations and sources of ambient fossil and biogenic-derived  
925 carbonaceous aerosols based on <sup>14</sup>C measurements in Lhasa, Tibet, *Atmos. Res.*,  
926 96, 553-559, <https://doi.org/10.1016/j.atmosres.2010.01.003>, 2010.

927 Huang, L., Brook, J. R., Zhang, W., Li, S. M., Graham, L., Ernst, D., Chivulescu, A.,  
928 and Lu, G.: Stable isotope measurements of carbon fractions (OC/EC) in  
929 airborne particulate: A new dimension for source characterization and  
930 apportionment, *Atmos. Environ.*, 40, 2690-2705,  
931 <https://doi.org/10.1016/j.atmosenv.2005.11.062>, 2006.

932 Huang, R. J., Zhang, Y. L., Bozzetti, C., Ho, K. F., Cao, J. J., Han, Y. M., Dällenbach,  
933 K. R., Slowik, J. G., Platt, S. M., Canonaco, F., Zotter, P., Wolf, R., Pieber, S. M.,  
934 Bruns, E. A., Crippa, M., Ciarelli, G., Piazzalunga, A., Schwikowski, M.,  
935 Abbaszade, G., Schnelle-Kreis, J., Zimmermann, R., An, Z., Szidat, S.,  
936 Baltensperger, U., Haddad, I. E., and Prévôt, A.: High secondary aerosol  
937 contribution to particulate pollution during haze events in China, *Nature*, 514,  
938 218-222, <https://doi.org/10.1038/nature13774>, 2014.

939 Jacobson, M. C., Hansson, H.-C., Noone, K. J., and Charlson, R. J.: Organic  
940 atmospheric aerosols: Review and state of the science, *Rev. Geophys.*, 38,  
941 267-294, <https://doi.org/10.1029/1998RG000045>, 2000.

942 Jacobson, M. Z.: Strong radiative heating due to the mixing state of black carbon in  
943 atmospheric aerosols, *Nature*, <https://doi.org/10.1038/35055518>, 2001.

944 Ji, D. S., Yan, Y. C., Wang, Z. S., He, J., Liu, B. X., Sun, Y., Gao, M., Li, Y., Cao, W.,  
945 Cui, Y., Hu, B., Xin, J. Y., Wang, L. L., Liu, Z. R., Tang, G. Q., and Wang, Y. S.:  
946 Two-year continuous measurements of carbonaceous aerosols in urban Beijing,  
947 China: Temporal variations, characteristics and source analyses, *Chemosphere*,  
948 200, 191-200, <https://doi.org/10.1016/j.chemosphere.2018.02.067>, 2018.

949 Jimenez, J. L., Canagaratna, M. R., Donahue, N. M., Prevot, A. S. H., Zhang, Q.,  
950 Kroll, J. H., DeCarlo, P. F., Allan, J. D., Coe, H., Ng, N. L., Aiken, A. C.,  
951 Docherty, K. S., Ulbrich, I. M., Grieshop, A. P., Robinson, A. L., Duplissy, J.,  
952 Smith, J. D., Wilson, K. R., Lanz, V. A., Hueglin, C., Sun, Y. L., Tian, J.,  
953 Laaksonen, A., Raatikainen, T., Rautiainen, J., Vaattovaara, P., Ehn, M., Kulmala,  
954 M., Tomlinson, J. M., Collins, D. R., Cubison, M. J., Dunlea, J., Huffman, J. A.,  
955 Onasch, T. B., Alfarra, M. R., Williams, P. I., Bower, K., Kondo, Y., Schneider, J.,  
956 Drewnick, F., Borrmann, S., Weimer, S., Demerjian, K., Salcedo, D., Cottrell, L.,  
957 Griffin, R., Takami, A., Miyoshi, T., Hatakeyama, S., Shimono, A., Sun, J. Y.,  
958 Zhang, Y. M., Dzepina, K., Kimmel, J. R., Sueper, D., Jayne, J. T., Herndon, S.  
959 C., Trimborn, A. M., Williams, L. R., Wood, E. C., Middlebrook, A. M., Kolb, C.  
960 E., Baltensperger, U., and Worsnop, D. R.: Evolution of Organic Aerosols in the  
961 Atmosphere, *Science*, 326, 1525-1529, <https://doi.org/10.1126/science.1180353>,  
962 2009.

963 Jull, A. J. T.: Radiocarbon dating| AMS method, in: *Encyclopedia of Quaternary*  
964 *science* 2911-2918, 2007.

965 Kawashima, H., and Haneishi, Y.: Effects of combustion emissions from the Eurasian  
966 continent in winter on seasonal  $\delta^{13}\text{C}$  of elemental carbon in aerosols in Japan,

967 Atmos. Environ., 46, 568-579, <https://doi.org/10.1016/j.atmosenv.2011.05.015>,  
968 2012.

969 Kiehl, J.: Twentieth century climate model response and climate sensitivity, *Geophys.*  
970 *Res. Lett.*, 34, 22710, <https://doi.org/10.1029/2007GL031383>, 2007.

971 Kirillova, E. N., Andersson, A., Sheesley, R. J., Kruså M., Praveen, P. S., Budhavant,  
972 K., Safai, P. D., Rao, P., and Gustafsson, Ö.: 13C- And 14C-based study of  
973 sources and atmospheric processing of water-soluble organic carbon (WSOC) in  
974 South Asian aerosols, *Journal of Geophysical Research Atmospheres*, 118,  
975 614-626, <https://doi.org/10.1002/jgrd.50130>, 2013.

976 Kumagai, K., Iijima, A., Shimoda, M., Saitoh, Y., Kozawa, K., Hagino, H., and  
977 Sakamoto, K.: Determination of Dicarboxylic Acids and Levoglucosan in Fine  
978 Particles in the Kanto Plain, Japan, for Source Apportionment of Organic  
979 Aerosols, *Aerosol Air Qual. Res.*, 10, 282-291,  
980 <https://doi.org/10.4209/aaqr.2009.11.0075>, 2010.

981 Levin, I., Kromer, B., Schmidt, M., and Sartorius, H.: A novel approach for  
982 independent budgeting of fossil fuel CO<sub>2</sub> over Europe by 14CO<sub>2</sub> observations,  
983 *Geophys. Res. Lett.*, 30, <https://doi.org/10.1029/2003GL018477>, 2003.

984 Levin, I., Naegler, T., Kromer, B., Diehl, M., Francey, R., Gomez Pelaez, A., Steele, P.,  
985 Wagenbach, D., Weller, R., and Worthy, D.: Observations and modelling of the  
986 global distribution and long-term trend of atmospheric 14CO<sub>2</sub>, *Tellus B*, 62,  
987 26-46, <https://doi.org/10.1111/j.1600-0889.2009.00446.x>, 2010.

988 Lewis, C. W., Klouda, G. A., and Ellenson, W. D.: Radiocarbon measurement of the  
989 biogenic contribution to summertime PM-2.5 ambient aerosol in Nashville, TN,  
990 *Atmos. Environ.*, 38, 6053-6061, <https://doi.org/10.1016/j.atmosenv.2004.06.011>,  
991 2004.

992 Li, C. L., Bosch, C., Kang, S. C., Andersson, A., Chen, P. F., Zhang, Q. G., Cong, Z.  
993 Y., Chen, B., Qin, D. H., and Gustafsson, Ö.: Sources of black carbon to the  
994 Himalayan-Tibetan Plateau glaciers, *Nat. Commun.*, 7, 12574,  
995 <https://doi.org/10.1038/ncomms12574>, 2016.

996 Li, H. M., Yang, Y., Wang, H. L., Li, B. J., Wang, P. Y., Li, J. D., and Liao, H.:  
997 Constructing a spatiotemporally coherent long-term PM<sub>2.5</sub> concentration dataset  
998 over China during 1980–2019 using a machine learning approach, *Sci. Total*  
999 *Environ.*, 765, 0048-9697, <https://doi.org/10.1016/j.scitotenv.2020.144263>,  
1000 2021a.

1001 Li, X. R., Wang, Y. S., Guo, X. Q., and Wang, Y. F.: Seasonal variation and source  
1002 apportionment of organic and inorganic compounds in PM<sub>2.5</sub> and PM<sub>10</sub>  
1003 particulates in Beijing, China, *J. Environ. Sci.*, 25, 741-750,  
1004 [https://doi.org/10.1016/S1001-0742\(12\)60121-1](https://doi.org/10.1016/S1001-0742(12)60121-1), 2013.

1005 Li, Y. M., Fu, T.-M., Yu, J. Z., Feng, X., Zhang, L. J., Chen, J., Boreddy, S. K. R.,  
1006 Kawamura, K., Fu, P., Yang, X., Zhu, L., and Zeng, Z. Z.: Impacts of chemical  
1007 degradation on the global budget of atmospheric levoglucosan and its use as a  
1008 biomass burning tracer, *Environ. Sci. Technol.*, 55, 5525-5536,  
1009 <https://doi.org/10.1021/acs.est.0c07313>, 2021b.

1010 Liao, C. P., Wu, C. Z., Yan, y. J., and Huang, H. T.: Chemical elemental characteristics  
1011 of biomass fuels in China, *Biomass Bioenergy*, 27, 119-130,  
1012 <https://doi.org/10.1016/j.biombioe.2004.01.002>, 2004.

1013 Lim, S., Yang, X., Lee, M., Li, G., Jeon, K., Lim, S. H., YangYang, X., Lee, M. H., Li,  
1014 G., Gao, Y. G., Shang, X. N., Zhang, K., I.Czimczik, C., Xu, X. M., Min-SukBae,  
1015 Moon, K.-J., and Jeon, K.: Fossil-driven secondary inorganic PM<sub>2.5</sub>  
1016 enhancement in the North China Plain: Evidence from carbon and nitrogen

1017 isotopes, Environ. Pollut., 266, 115163,  
1018 <https://doi.org/10.1016/j.envpol.2020.115163>, 2020.

1019 Liu, D., Li, J., Zhang, Y. L., Xu, Y., Liu, X., Ping, D., Shen, C. D., Chen, Y. J., Tian,  
1020 C., and Zhang, G.: The Use of Levoglucosan and Radiocarbon for Source  
1021 Apportionment of PM<sub>2.5</sub> Carbonaceous Aerosols at a Background Site in East  
1022 China, Environ. Sci. Technol., 47, <https://doi.org/10.1021/es401250k>, 2013.

1023 Liu, J., Mo, Y., Li, J., Liu, D., Shen, C., Ding, P., Jiang, H., Cheng, Z., Zhang, X., and  
1024 Tian, C.: Radiocarbon - derived source apportionment of fine carbonaceous  
1025 aerosols before, during, and after the 2014 Asia - Pacific Economic Cooperation  
1026 (APEC) summit in Beijing, China, J. Geophys. Res.: Atmos., 121, 4177-4187,  
1027 <https://doi.org/10.5194/acp-16-2985-2016>, 2016a.

1028 Liu, J. W., Li, J., Liu, D., Ding, P., Shen, C. D., Mo, Y. Z., Wang, X. M., Luo, C. L.,  
1029 Cheng, Z. N., Szidat, S., Zhang, Y. L., Chen, Y. J., and Zhang, G.: Source  
1030 apportionment and dynamic changes of carbonaceous aerosols during the haze  
1031 bloom-decay process in China based on radiocarbon and organic molecular tracer,  
1032 Atmos. Chem. Phys., 16, 2985–2996, <https://doi.org/10.5194/acp-16-2985-2016>,  
1033 2016b.

1034 Liu, Y., Shao, M., Fu, L. L., Lu, S. H., Zeng, L. M., and Tang, D. G.: Source profiles  
1035 of volatile organic compounds (VOCs) measured in China: Part I, Atmos.  
1036 Environ., 42, 6247-6260, <https://doi.org/10.1016/j.atmosenv.2008.01.070>, 2008.

1037 Liu, Z. R., Hu, B., Liu, Q., Sun, Y., and Wang, Y. S.: Source apportionment of urban  
1038 fine particle number concentration during summertime in Beijing, Atmos.  
1039 Environ., 96, 359-369, <https://doi.org/10.1016/j.atmosenv.2014.06.055>, 2014.

1040 Locker, H. B.: The use of levoglucosan to assess the environmental impact of  
1041 residential wood-burning on air quality, Hanover, NH (US); Dartmouth College,

1042 1988.

1043 Lopez-Veneroni, D.: The stable carbon isotope composition of PM<sub>2.5</sub> and PM<sub>10</sub> in  
1044 Mexico City Metropolitan Area air, *Atmos. Environ.*, 43, 4491-4502,  
1045 <https://doi.org/10.1016/j.atmosenv.2009.06.036>, 2009.

1046 Lu, L., Tang, Y., Xie, J. S., and Yuan, Y. L.: The role of marginal agricultural  
1047 land-based mulberry planting in biomass energy production, *Renewable Energy*,  
1048 34, 1789-1794, <https://doi.org/10.1016/j.renene.2008.12.017>, 2009.

1049 Martinelli, L. A., Camargo, P. B., Lara, L., Victoria, R. L., and Artaxo, P.: Stable  
1050 carbon and nitrogen isotopic composition of bulk aerosol particles in a C<sub>4</sub> plant  
1051 landscape of southeast Brazil, *Atmos. Environ.*, 36, 2427-2432,  
1052 [https://doi.org/10.1016/S1352-2310\(01\)00454-X](https://doi.org/10.1016/S1352-2310(01)00454-X), 2002.

1053 MEE: (Ministry of Ecology and Environment of the People's Republic of China):  
1054 Technical Regulation on Ambient Air Quality Index, China Environmental  
1055 Science Press (HJ 633-2012),  
1056 [http://www.mee.gov.cn/ywgz/fgbz/bz/bzwb/jcffbz/201203/t20120302\\_224166.sh](http://www.mee.gov.cn/ywgz/fgbz/bz/bzwb/jcffbz/201203/t20120302_224166.shtml)  
1057 [tml](http://www.mee.gov.cn/ywgz/fgbz/bz/bzwb/jcffbz/201203/t20120302_224166.shtml), 2012 (last access: 28 March 2022).

1058 MEE: (Ministry of Ecology and Environment of the People's Republic of China):  
1059 Bulletin of Ecology and Environment of the People's Republic of China 2013,  
1060 [http://www.mee.gov.cn/hjzl/sthjzk/zghjzkgb/201605/P020160526564730573906.](http://www.mee.gov.cn/hjzl/sthjzk/zghjzkgb/201605/P020160526564730573906.pdf)  
1061 [pdf](http://www.mee.gov.cn/hjzl/sthjzk/zghjzkgb/201605/P020160526564730573906.pdf), 2014 (last access: 28 March 2022).

1062 MEE: (Ministry of Ecology and Environment of the People's Republic of China):  
1063 Bulletin of Ecology and Environment of the People's Republic of China 2018,  
1064 [http://www.mee.gov.cn/hjzl/sthjzk/zghjzkgb/201905/P020190619587632630618.](http://www.mee.gov.cn/hjzl/sthjzk/zghjzkgb/201905/P020190619587632630618.pdf)  
1065 [pdf](http://www.mee.gov.cn/hjzl/sthjzk/zghjzkgb/201905/P020190619587632630618.pdf), 2019 (last access: 28 March 2022).

1066 MEE: (Ministry of Ecology and Environment of the People's Republic of China):

1067 Bulletin of Ecology and Environment of the People's Republic of China 2019,  
1068 [http://www.mee.gov.cn/hjzl/sthjzk/zghjzkgb/202006/P020200602509464172096.](http://www.mee.gov.cn/hjzl/sthjzk/zghjzkgb/202006/P020200602509464172096.pdf)  
1069 [pdf](http://www.mee.gov.cn/hjzl/sthjzk/zghjzkgb/202006/P020200602509464172096.pdf), 2020 (last access: 28 March 2022).

1070 MEE: (Ministry of Ecology and Environment of the People's Republic of China):  
1071 Bulletin of Ecology and Environment of the People's Republic of China 2020,  
1072 [http://www.mee.gov.cn/hjzl/sthjzk/zghjzkgb/202105/P020210526572756184785.](http://www.mee.gov.cn/hjzl/sthjzk/zghjzkgb/202105/P020210526572756184785.pdf)  
1073 [pdf](http://www.mee.gov.cn/hjzl/sthjzk/zghjzkgb/202105/P020210526572756184785.pdf), 2021 (last access: 28 March 2022).

1074 Mook, W. G., and Plicht, J. V. D.: Reporting 14C Activities and Concentrations,  
1075 Radiocarbon, 41, 227-239, <https://doi.org/10.1017/S0033822200057106>, 1999.

1076 Moura, J. M. S., Martens, C. S., Moreira, M. Z., Lima, R. L., Sampaio, I. C. G.,  
1077 Mendlovitz, H. P., and Menton, M. C.: Spatial and seasonal variations in the  
1078 stable carbon isotopic composition of methane in stream sediments of eastern  
1079 Amazonia, Tellus B, 60, 21-31,  
1080 <https://doi.org/10.1111/j.1600-0889.2007.00322.x>, 2008.

1081 NBS: (National bureau of statistics): China Statistical Yearbook-2019, China Statistics  
1082 press <http://www.stats.gov.cn/tjsj/ndsj/2019/indexch.htm>, 2020 (last access: 28  
1083 March 2022).

1084 NBS: (National bureau of statistics): China Statistical Yearbook-2020, China Statistics  
1085 press, <http://www.stats.gov.cn/tjsj/ndsj/2020/indexch.htm>, 2021 (last access: 28  
1086 March 2022).

1087 Ni, H. Y., Huang, R. J., Cao, J. J., Liu, W. G., Zhang, T., Wang, M., Meijer, H. A., and  
1088 Dusek, U.: Source apportionment of carbonaceous aerosols in Xi'an, China:  
1089 insights from a full year of measurements of radiocarbon and the stable isotope  
1090 C-13, Atmos. Chem. Phys., <https://doi.org/10.5194/acp-18-16363-2018>, 2018.

1091 Ni, H. Y., Huang, R. J., Cosijn, M. M., Yang, L., and Dusek, U.: Measurement report:



1092 dual-carbon isotopic characterization of carbonaceous aerosol reveals different  
1093 primary and secondary sources in Beijing and Xi'an during severe haze events,  
1094 *Atmos. Chem. Phys.*, **20**, 16041-16053,  
1095 <https://doi.org/10.5194/acp-20-16041-2020>, 2020.

1096 Niu, Z. C., Wang, S., Chen, J. S., Zhang, F. W., Chen, X. Q., He, C., Lin, L. F., Yin, L.  
1097 Q., and Xu, L. L.: Source contributions to carbonaceous species in PM<sub>2.5</sub> and  
1098 their uncertainty analysis at typical urban, peri-urban and background sites in  
1099 southeast China, *Environ. Pollut.*, **181**, 107-114,  
1100 <https://doi.org/10.1016/j.envpol.2013.06.006>, 2013.

1101 Niu, Z. C., Zhou, W. J., Cheng, P., Wu, S. G., Lu, X. F., Xiong, X. H., Du, H., and Fu,  
1102 Y. C.: Observations of Atmospheric  $\Delta^{14}\text{C}$  at the Global and Regional  
1103 Background Sites in China: Implication for Fossil Fuel CO<sub>2</sub> Inputs, *Environ.*  
1104 *Sci. Technol.*, **50**, 12122-12128, <https://doi.org/10.1021/acs.est.6b02814>, 2016.

1105 Niu, Z. C., Feng, X., Zhou, W. J., Wang, P., Liu, Y., Lu, X. F., Du, H., Fu, Y. C., Li, M.,  
1106 Mei, R. C., Li, Q., and Cai, Q. F.: Tree-ring  $\Delta^{14}\text{C}$  time series from 1948 to  
1107 2018 at a regional background site, China: Influences of atmospheric nuclear  
1108 weapons tests and fossil fuel emissions, *Atmos. Environ.*, **246**,  
1109 <https://doi.org/10.1016/j.atmosenv.2020.118156>, 2021.

1110 Novakov, T., Menon, S., Kirchstetter, T. W., Koch, D., and Hansen, J. E.: Aerosol  
1111 organic carbon to black carbon ratios: Analysis of published data and  
1112 implications for climate forcing, *Journal of Geophysical Research Atmospheres*,  
1113 **110**, <https://doi.org/10.1029/2005JD005977>, 2005.

1114 Oros, D. R., and Simoneit, B. R. T.: Identification and emission factors of molecular  
1115 tracers in organic aerosols from biomass burning Part 2. Deciduous trees, *Appl.*  
1116 *Geochem.*, **16**, 1545-1565, [https://doi.org/10.1016/s0883-2927\(01\)00022-1](https://doi.org/10.1016/s0883-2927(01)00022-1),

1117 2001a.

1118 Oros, D. R., and Simoneit, B. R. T.: Identification and emission factors of molecular  
1119 tracers in organic aerosols from biomass burning Part 1. Temperate climate  
1120 conifers, *Appl. Geochem.*, 16, 1513-1544,  
1121 [https://doi.org/10.1016/s0883-2927\(01\)00021-x](https://doi.org/10.1016/s0883-2927(01)00021-x), 2001b.

1122 PGHP: (The People's Government of Hebei Province): Hebei Economic  
1123 Yearbook-2020, China Statistics press,  
1124 <http://tjj.hebei.gov.cn/hetj/tjnj/2020/indexch.htm>, 2021 (last access: 28 March  
1125 2022).

1126 Popovicheva, O. B., Kozlov, V. S., Engling, G., Diapouli, E., Persiantseva, N. M.,  
1127 Timofeev, M. A., Fan, T.-S., Saraga, D., and Eleftheriadis, K.: Small-scale study  
1128 of siberian biomass burning: i. smoke microstructure, *Aerosol Air Qual. Res.*, 15,  
1129 117-128, <https://doi.org/10.4209/aaqr.2014.09.0206>, 2014.

1130 Pugliese, S. C., Murphy, J. G., Vogel, F., and Worthy, D.: Characterization of the  $\delta^{13}C$   
1131 signatures of anthropogenic CO<sub>2</sub> emissions in the Greater Toronto Area, Canada,  
1132 *Appl. Geochem.*, 83, 171-1800,  
1133 <https://doi.org/10.1016/j.apgeochem.2016.11.003>, 2017.

1134 Puxbaum, H., Caseiro, A., Sánchez-Ochoa, A., Kasper-Giebl, A., Claeys, M.,  
1135 Gelencsér, A., Legrand, M., Preunkert, S., and Pio, C.: Levoglucosan levels at  
1136 background sites in Europe for assessing the impact of biomass combustion on  
1137 the European aerosol background, *J. Geophys. Res.*, 112, D23S05,  
1138 <https://doi.org/10.1029/2006jd008114>, 2007.

1139 Rajput, P., Sarin, M. M., Rengarajan, R., and Singh, D.: Atmospheric polycyclic  
1140 aromatic hydrocarbons (pahs) from post-harvest biomass burning emissions in  
1141 the indo-gangetic plain: isomer ratios and temporal trends, *Atmospheric*

1142 Environment, 45, 6732-6740, <https://doi.org/10.1016/j.atmosenv.2011.08.018>,  
1143 2011.

1144 SAPBS: (Shaanxi Provincial Bureau of Statistics): Shaanxi Statistical Yearbook-2020,  
1145 China Statistics press, <http://tjj.shaanxi.gov.cn/upload/n2020/indexch.htm>, 2020  
1146 (last access: 28 March 2022).

1147 Seinfeld, J. H., and Pandis, S. N.: Atmospheric Chemistry and Physics: From Air  
1148 Pollution to Climate Change, Environ.: Sci. Policy Sustainable Dev., 1998.

1149 Shang, J., Khuzestani, R. B., Tian, J., Schauer, J. J., Hua, J., Zhang, Y., Cai, T., Fang,  
1150 D., An, J., and Zhang, Y.: Chemical characterization and source apportionment of  
1151 PM<sub>2.5</sub> personal exposure of two cohorts living in urban and suburban Beijing,  
1152 Environ. Pollut., <https://doi.org/10.1016/j.envpol.2018.11.076>, 2019.

1153 Shao, M., Li, J., and Tang, X.: The application of accelerator mass spectrometry  
1154 (AMS) in the study of source identification of aerosols (in Chinese). Acta  
1155 Scientiae Circumstantiae 16 (2), 130–141, 1996.

1156 Shen, G. F., Wang, W., Yang, Y. F., Zhu, C., Min, Y. J., Xue, M., Ding, J. N., Li, W.,  
1157 Wang, B., Shen, H. Z., Wang, R., Wang, X. L., and Tao, S.: Emission factors and  
1158 particulate matter size distribution of polycyclic aromatic hydrocarbons from  
1159 residential coal combustions in rural Northern China, Atmos. Environ., 44,  
1160 5237-5243, <https://doi.org/10.1016/j.atmosenv.2010.08.042>, 2010.

1161 Shen, Z. X., Cao, J. J., Liu, S. X., Zhu, C. S., Wang, X., Zhang, T., Xu, H. M., and Hu,  
1162 T. F.: Chemical Composition of PM<sub>10</sub> and PM<sub>2.5</sub> Collected at Ground Level and  
1163 100 Meters during a Strong Winter-Time Pollution Episode in Xi'an, China, J.  
1164 Air Waste Manage. Assoc., <https://doi.org/10.1080/10473289.2011.608619>,  
1165 2011.

1166 Simoneit, B. R. T., Schauer, J. J., Nolte, C. G., Oros, D. R., Elias, V. O., Fraser, M. P.,

1167 Rogge, W. F., and Cass, G. R.: Levoglucosan, a tracer for cellulose in biomass  
1168 burning and atmospheric particles, *Atmos. Environ.*, 33, 173-182,  
1169 [https://doi.org/10.1016/S1352-2310\(98\)00145-9](https://doi.org/10.1016/S1352-2310(98)00145-9), 1999.

1170 Simpson, D., Yttri, K. E., Klimont, Z., Kupiainen, K., Caseiro, A., Gelencs ́r, A., Pio,  
1171 C., Puxbaum, H., and Legrand, M.: Modeling carbonaceous aerosol over Europe:  
1172 Analysis of the CARBOSOL and EMEP EC/OC campaigns, *Journal of*  
1173 *Geophysical Research Atmospheres*, 112, -,  
1174 <https://doi.org/10.1029/2006JD008158>, 2007.

1175 Slota, P. J., Jull, A. J. T., Linick, T. W., and Toolin, L. J.: Preparation of Small Samples  
1176 for <sup>14</sup>C Accelerator Targets by Catalytic Reduction of CO, *Radiocarbon*, 29,  
1177 303-306, <https://doi.org/10.1017/S0033822200056988>, 1987.

1178 Smith, B. N., and Epstein, S.: Two Categories of <sup>13</sup>C/<sup>12</sup>C Ratios for Higher Plants,  
1179 *Plant Physiol.*, 47, 380-384, <https://doi.org/10.1029/2006JD008158>, 1971.

1180 Song, Y., Zhang, Y. H., Xie, S. D., Zeng, L. M., Zheng, M., Salmon, L., Shao, M., and  
1181 Slanina, S.: Source apportionment of PM<sub>2.5</sub> in Beijing by positive matrix  
1182 factorization, *Atmos. Environ.*, 40, 1526-1537,  
1183 <https://doi.org/10.1016/j.atmosenv.2005.10.039>, 2006.

1184 SPBS: (Shanxi Provincial Bureau of Statistics): Shanxi Statistical Yearbook-2019,  
1185 China Statistics press,  
1186 <http://tjj.shaanxi.gov.cn/upload/2020/pro/3sxtjnj/zk/indexch.htm>, 2020 (last  
1187 access: 28 March 2022).

1188 Streets, D. G., Bond, T. C., Carmichael, G. R., Fernandes, S. D., Fu, Q., He, D.,  
1189 Klimont, Z., Nelson, S. M., Tsai, N. Y., Wang, M. Q., Woo, J. H., and Yarber, K.  
1190 F.: An inventory of gaseous and primary aerosol emissions in Asia in the year  
1191 2000, *J. Geophys. Res.: Atmos.*, 108, <https://doi.org/10.1029/2002JD003093>,

1192 2003a.

1193 Streets, D. G., Yarber, K. F., Woo, J.-H., and Carmichael, G. R.: Biomass burning in  
1194 Asia: Annual and seasonal estimates and atmospheric emissions, *Global*  
1195 *Biogeochem. Cycles*, 17, 1099, <https://doi.org/10.1029/2003GB002040>, 2003b.

1196 Stuiver, M., and Polach, H.: Discussion: Reporting of  $^{14}\text{C}$  data, *Radiocarbon*, 19,  
1197 355-363, <https://doi.org/10.1017/S0033822200003672>, 1977.

1198 Sun, X. S., Hu, M., Guo, S., Liu, K. X., and Zhou, L. P.:  $^{14}\text{C}$ -Based source  
1199 assessment of carbonaceous aerosols at a rural site, *Atmos. Environ.*, 50, 36-40,  
1200 <https://doi.org/10.1016/j.atmosenv.2012.01.008>, 2012.

1201 Sun, Y. L., Zhuang, G. S., Tang, A. H., Wang, Y., and An, Z. S.: Chemical  
1202 characteristics of  $\text{PM}_{2.5}$  and  $\text{PM}_{10}$  in haze-fog episodes in Beijing, *Environ. Sci.*  
1203 *Technol.*, 40, 3148-3155, <https://doi.org/10.1021/es051533g>, 2006.

1204 Szidat, S., Jenk, T. M., Gaeggeler, H. W., Synal, H. A., Hajdas, I., Bonani, G., and  
1205 Saurer, M.: THEODORE, a two-step heating system for the EC/OC  
1206 determination of radiocarbon ( $^{14}\text{C}$ ) in the environment, *Nucl. Instrum. Methods*  
1207 *Phys. Res.*, 223, 829-836, <https://doi.org/10.1016/j.nimb.2004.04.153>, 2004.

1208 Szidat, S., Jenk, T. M., Synal, H., Kalberer, M., Wacker, L., Hajdas, I., Kasper - Giebl,  
1209 A., and Baltensperger, U.: Contributions of fossil fuel, biomass burning, and  
1210 biogenic emissions to carbonaceous aerosols in Zürich as traced by  $^{14}\text{C}$ , *Journal*  
1211 *of Geophysical Research Atmospheres*, 111, -,  
1212 <http://doi.org/10.1029/2005JD006590>, 2006.

1213 Szidat, S., Ruff, M., Perron, N., Wacker, L., Synal, H. A., Hallquist, M., Shannigrahi,  
1214 A. S., Yttri, K., Dye, C., and Simpson, D.: Fossil and non-fossil sources of  
1215 organic carbon (OC) and elemental carbon (EC) in Göteborg, Sweden, *Atmos.*  
1216 *Chem. Phys.*, 9, 16255-16289, <https://doi.org/10.5194/acpd-8-16255-2008>, 2009.

1217 Tanarit, S., Alex, G., Detlev, H., Jana, M., and Christine, W.: Secondary Organic  
1218 Aerosol from Sesquiterpene and Monoterpene Emissions in the United States,  
1219 Environ. Sci. Technol., 42, 8784–8790, <https://doi.org/10.1021/es800817r>, 2008.

1220 Tian, S. L., Pan, Y. P., and Wang, Y. S.: Size-resolved source apportionment of  
1221 particulate matter in urban Beijing during haze and non-haze episodes, Atmos.  
1222 Chem. Phys., 16, 9405-9443, <https://doi.org/10.5194/acp-16-1-2016>, 2016.

1223 Turekian, V. C., Macko, S., Ballentine, D., Swap, R. J., and Garstang, M.: Causes of  
1224 bulk carbon and nitrogen isotopic fractionations in the products of vegetation  
1225 burns: laboratory studies, Chem. Geol., 152, 181-192,  
1226 [https://doi.org/10.1016/S0009-2541\(98\)00105-3](https://doi.org/10.1016/S0009-2541(98)00105-3), 1998.

1227 Turnbull, J. C., Lehman, S. J., Miller, J. B., Sparks, R. J., Southon, J. R., and Tans, P.  
1228 P.: A new high precision  $^{14}\text{C}$  time series for North American continental air, J.  
1229 Geophys. Res., <http://doi.org/10.1029/2006jd008184>, 2007.

1230 Turpin, B. J., and Huntzicker, J. J.: Identification of secondary organic aerosol  
1231 episodes and quantitation of primary and secondary organic aerosol  
1232 concentrations during SCAQS, Atmos. Environ., 29, 3527-3544,  
1233 [https://doi.org/10.1016/1352-2310\(94\)00276-Q](https://doi.org/10.1016/1352-2310(94)00276-Q), 1995.

1234 Vardag, S. N., Gerbig, C., Janssens-Maenhout, G., and Levin, I.: Estimation of  
1235 continuous anthropogenic  $\text{CO}_2$ : model-based evaluation of  $\text{CO}_2$ ,  $\text{CO}$ ,  
1236  $\text{D}^{13}\text{C}(\text{CO}_2)$  and  $\text{D}^{14}\text{C}(\text{CO}_2)$  tracer methods, Atmos. Chem. Phys., 15,  
1237 12705–12729, <https://doi.org/10.5194/acp-15-12705-2015>, 2015.

1238 Vonwiller, M., Quintero, G. S., and Szidat, S.: Isolation and  $^{14}\text{C}$  analysis of  
1239 humic-like substances (HULIS) from ambient aerosol samples,  
1240 <https://doi.org/10.7892/boris.108864>, 2017.

1241 Wang, G., Cheng, S., Li, J., Lang, J., Wen, W., Yang, X., Tian, L., Wang, G., Cheng, S.

1242 Y., Li, J. B., Lang, J. L., Wen, W., Yang, X. W., and Tian, L.: Source  
1243 apportionment and seasonal variation of PM<sub>2.5</sub> carbonaceous aerosol in the  
1244 Beijing-Tianjin-Hebei Region of China, *Environ. Monit. Assess.*, 187, 1-13,  
1245 <https://doi.org/10.1007/s10661-015-4288-x>, 2015.

1246 Wang, H. L., Zhuang, Y. H., Wang, Y., Yuan, Y. L., and Zhuang, G. S.: Long-term  
1247 monitoring and source apportionment of PM<sub>2.5</sub>/PM<sub>10</sub> in Beijing, China, *J.*  
1248 *Environ. Sci.*, 20, 1323-1327, [https://doi.org/10.1016/S1001-0742\(08\)62228-7](https://doi.org/10.1016/S1001-0742(08)62228-7),  
1249 2008.

1250 Wang, X. F., Zhu, G. H., Wu, Y. G., and Shen, X. Y.: Chemical composition and size  
1251 distribution of particles in the atmosphere in north part of Beijing city for winter  
1252 and summer (In Chinese), *Chinese Journal of Atmospheric Sciences*, 14, 199-206,  
1253 <https://doi.org/10.3878/j.issn.1006-9895.1990.02.09>, 1990.

1254 Wang, Z. Z., Bi, X. H., Sheng, G. Y., and Fu, J. M.: Characterization of organic  
1255 compounds and molecular tracers from biomass burning smoke in South China I:  
1256 Broad-leaf trees and shrubs, *Atmos. Environ.*, 43, 3096-3102,  
1257 <https://doi.org/10.1016/j.atmosenv.2009.03.012>, 2009.

1258 Weber, R. J., Sullivan, A. P., Peltier, R. E., Russell, A., Yan, B., Zheng, M., Gouw, J.  
1259 D., Warneke, C., Brock, C., and Holloway, J. S.: A study of secondary organic  
1260 aerosol formation in the anthropogenic-influenced southeastern United States,  
1261 *Journal of Geophysical Research Atmospheres*, 112, D13302,  
1262 <https://doi.org/10.1029/2007jd008408>, 2007.

1263 Widory, D.: Combustibles, fuels and their combustion products: A view through  
1264 carbon isotopes, *Combust. Theor. Model.*, 10, 831-841,  
1265 <https://doi.org/10.1080/13647830600720264>, 2006.

1266 Winiger, P., Andersson, A., Eckhardt, S., Stohl, A., Semiletov, I. P., Dudarev, O. V.,

1267 Charkin, A., Shakhova, N., Klimont, Z., and Heyes, C.: Siberian Arctic black  
1268 carbon sources constrained by model and observation, Proc Natl Acad Sci U S A,  
1269 114, E1054, <https://doi.org/10.1073/pnas.1613401114>, 2017.

1270 Wu, J., Kong, S. F., Zeng, X., Cheng, Y., Yan, Q., Zheng, H., Yan, Y. Y., Zheng, S. R.,  
1271 Liu, D. T., Zhang, X. Y., Fu, P. Q., Wang, S. X., and Qi, S. H.: First  
1272 High-Resolution Emission Inventory of Levoglucosan for Biomass Burning and  
1273 Non-Biomass Burning Sources in China, Environ. Sci. Technol., 55, 1497-1507,  
1274 <https://doi.org/10.1021/acs.est.0c06675>, 2021.

1275 XAMBS: (Xi'an Municipal Bureau Statistics): Xi'an Statistical Yearbook-2014,  
1276 China Statistics press, <http://tjj.xa.gov.cn/tjnj/2014/tjnj/indexch.htm>, 2014 (last  
1277 access: 28 March 2022).

1278 XAMBS: (Xi'an Municipal Bureau Statistics): Xi'an Statistical Yearbook-2020 China  
1279 Statistics press, <http://tjj.xa.gov.cn/tjnj/2020/zk/indexch.htm>, 2021 (last access:  
1280 28 March 2022).

1281 Yan, X. Y., Ohara, T., and Akimoto, H.: Bottom-up estimate of biomass burning in  
1282 mainland china, Atmos. Environ., 40, 5262-5273,  
1283 <https://doi.org/10.1016/j.atmosenv.2006.04.040>, 2006.

1284 Yan, X. Y., and Crookes, R. J.: Energy demand and emissions from road  
1285 transportation vehicles in China, Prog. Energy Combust. Sci., 36, 651-676,  
1286 <https://doi.org/10.1016/j.pecs.2010.02.003>, 2010.

1287 Yang, F., He, K., Ye, B., Chen, X., Cha, L., Cadle, S. H., Chan, T., and Mulawa, P. A.:  
1288 One-year record of organic and elemental carbon in fine particles in downtown  
1289 Beijing and Shanghai, Atmos. Chem. Phys., 5, 1449-1457,  
1290 <https://doi.org/10.5194/acp-5-1449-2005>, 2005.

1291 Zhang, R., Jing, J., Tao, J., Hsu, S. C., Wang, G., Cao, J., Lee, C. S. L., Zhu, L., Chen,



1292 Z., and Zhao, Y.: Chemical characterization and source apportionment of PM<sub>2.5</sub>  
1293 in Beijing: seasonal perspective, *Atmos. Chem. Phys.*, 13, 7053-7074,  
1294 <https://doi.org/10.5194/acp-14-175-2014>, 2014.

1295 Zhang, Y. L., Perron, N., Ciobanu, V. G., Zotter, P., and Szidat, S.: On the isolation of  
1296 OC and EC and the optimal strategy of radiocarbon-based source apportionment  
1297 of carbonaceous aerosols, *Soil Biol. Biochem.*, 12, 17657-17702,  
1298 <https://doi.org/10.5194/acpd-12-17657-2012>, 2012.

1299 Zhang, Y. L., Huang, R. J., Haddad, I. E. I., Ho, K. F., Cao, J. J., Han, Y., Zotter, P.,  
1300 Bozzetti, C., Daellenbach, K. R., Canonaco, F., Slowik, J. G., Salazar, G.,  
1301 Schwikowski, M., Schnelle-Kreis, J., Abbaszade, G., Zimmermann, R.,  
1302 Baltensperger, U., Prévôt, A. S. H., and Szidat, S.: Fossil vs. non-fossil sources  
1303 of fine carbonaceous aerosols in four Chinese cities during the extreme winter  
1304 haze episode of 2013, *Atmos. Chem. Phys.*, 15, 1299-1312,  
1305 <https://doi.org/10.5194/acp-15-1299-2015>, 2015.

1306 Zhang, Y. L., Ren, H., Sun, Y. L., Cao, F., Chang, Y. H., Liu, S. D., Lee, X. H., Agrios,  
1307 K., Kawamura, K., Liu, D., Ren, L. J., Du, W., Wang, Z. F., Prévôt, A. S. H.,  
1308 Szidat, S., and Fu, P. Q.: High Contribution of Nonfossil Sources to  
1309 Submicrometer Organic Aerosols in Beijing, China, *Environ. Sci. Technol.*, 51,  
1310 7842, <https://doi.org/10.1021/acs.est.7b01517>, 2017a.

1311 Zhang, Y. X., Shao, M., Zhang, Y. H., Zeng, L. M., HE., L. Y., Zhu, B., Wei, Y. J., and  
1312 Zhu, X. L.: Source profiles of particulate organic matters emitted from cereal  
1313 straw burnings, *J. Environ. Sci.*, 19, 167-175,  
1314 [https://doi.org/10.1016/S1001-0742\(07\)60027-8](https://doi.org/10.1016/S1001-0742(07)60027-8), 2007.

1315 Zhang, Z. S., Engling, G., Chan, C. Y., Yang, Y. H., Lin, M., Shi, S., He, J., Li, Y. D.,  
1316 and Wang, X. M.: Determination of isoprene-derived secondary organic aerosol

1317 tracers (2-methyltetrols) by HPAEC-PAD: Results from size-resolved aerosols in  
1318 a tropical rainforest, *Atmos. Environ.*, 70, 468-476,  
1319 <https://doi.org/10.1016/j.atmosenv.2013.01.020>, 2013.

1320 Zhang, Z. S., Gao, J., Zhang, L. M., Wang, H., Tao, J., Qiu, X. H., Chai, F. H., Li, Y.,  
1321 and Wang, S. L.: Observations of biomass burning tracers in pm 2.5 at two  
1322 megacities in north china during 2014 apec summit, *Atmos. Environ.*, 169, 54-65,  
1323 <http://dx.doi.org/10.1016/j.atmosenv.2017.09.011>, 2017b.

1324 Zhao, P. S., Dong, F., Yang, Y. D., He, D., Zhao, X. J., Zhang, W. Z., Yao, Q., and Liu,  
1325 H. Y.: Characteristics of carbonaceous aerosol in the region of Beijing, Tianjin,  
1326 and Hebei, China, *Atmos. Environ.*, 71, 389–398,  
1327 <https://doi.org/10.1016/j.atmosenv.2013.02.010>, 2013.

1328 Zhao, Z. Z., Cao, J. J., Zhang, T., XingShen, Z., Ni, H. Y., Tian, J., Wang, Q. Y., Liu, S.  
1329 X., Zhou, J. M., Gu, J., and Shen, G. Z.: Stable carbon isotopes and levoglucosan  
1330 for pm 2.5 elemental carbon source apportionments in the largest city of  
1331 northwest china, *Atmos. Environ.*, 185, 253-261,  
1332 <https://doi.org/10.1016/j.atmosenv.2018.05.008>, 2018.

1333 Zhi, G. R., Chen, Y. J., Feng, Y. L., Xiong, S. C., Jun, L. I., Zhang, G., Sheng, G. Y.,  
1334 and Jiamo, F. U.: Emission characteristics of carbonaceous particles from various  
1335 residential coal-stoves in China, *Environ. Sci. Technol.*, 42, 3310,  
1336 <https://doi.org/10.1021/es702247q>, 2008.

1337 Zhou, W. J., Zhao, X. L., Feng, L. X., Lin, L., Kun, W. Z., Peng, C., Nian, Z. W., and  
1338 Hai, H. C.: The 3MV multi-element AMS in Xi'an, China: Unique features and  
1339 preliminary tests, *Radiocarbon*, 48, 285-293,  
1340 <https://doi.org/10.1017/S0033822200066492>, 2006.

1341 Zhou, W. J., Lua, X. F., Wu, Z. K., Zhao, W. N., Huang, C. H., Lia, L. L., Chen, P.,

1342 and Xin, Z. H.: New results on Xi'an-AMS and sample preparation systems at  
1343 Xi'an-AMS center, Nucl. Instrum. Methods Phys. Res., 262, 135-142,  
1344 <https://doi.org/10.1016/j.nimb.2007.04.221>, 2007.

1345 Zhou, W. J., Wu, S. G., Huo, W. W., Xiong, X. H., Cheng, P., Lu, X. F., and Niu, Z. C.:  
1346 Tracing fossil fuel CO<sub>2</sub> using  $\Delta^{14}\text{C}$  in Xi'an City, China, Atmos. Environ., 94,  
1347 538-545, <https://doi.org/10.1017/S0033822200066492>, 2014.

1348